Tracing foot-and-mouth disease virus phylogeographical patterns and transmission dynamics.

Running title: Phylogeography of foot-and-mouth disease virus

Manuel Jara[1], Alba Frias-De-Diego[1], Simon Dellicour[2,3], Guy Baele[3], and Gustavo Machado[1,*]

[1]Department of Population Health and Pathobiology, College of Veterinary Medicine, North Carolina State University, Raleigh, NC, USA

[2]Spatial Epidemiology Lab (SpELL), Université Libre de Bruxelles, CP160/12 50, av. FD Roosevelt, 1050 Bruxelles, Belgium

[3]Department of Microbiology, Immunology and Transplantation, Laboratory for Clinical and Epidemiological Virology, Rega Institute, KU Leuven, Herestraat 49, 3000 Leuven, Belgium

[*]Corresponding author: gmachad@ncsu.edu

Abstract

Foot-and-mouth disease virus (FMDV) has proven its potential to propagate across local and international borders on numerous occasions, but yet details about the directionality of the spread along with the role of the different host in transmission remain unexplored. To elucidate FMDV global spread characteristics, we studied the spatiotemporal phylodynamics of serotypes O, A, Asia1, SAT1, SAT2, and SAT3, based on more than 50 years of phylogenetic and epidemiological information. Our results revealed phylogeographic patterns, dispersal rates, and the role of host species in the dispersal and maintenance of virus circulation. Contrary to previous studies, our results showed that three serotypes were monophyletic (O, A, and Asia1), while all SATs serotypes did not evidence a defined common ancestor. Root state posterior probability (RSPP) analysis suggested Belgium as the country of origin for serotype O (RSPP=

0.27). India was the ancestral country for serotypes A (RSPP= 0.28), and Asia-1 (RSPP= 0.34), while Uganda appeared as the most likely origin country of all SAT serotypes (RSPP> 0.45). Furthermore, we identified the key centers of dispersal of the virus, being China, India and Uganda the most important ones. Bayes factor analysis revealed cattle as the major source of the virus for most of the serotypes (RSPP> 0.63), where the most important host-species transition route for serotypes O, A, and Asia1 was from cattle *Bos taurus* to swine *Sus scrofa domesticus* (BF>500), while, for SAT serotypes was from *B. taurus* to African buffalo *Syncerus caffer*. This study provides significant insights into the spatiotemporal dynamics of the global circulation of FMDV serotypes, by characterizing the viral routes of spread at serotype level, especially uncovering the importance of host species for each serotype in the evolution and spread of FMDV which further improve future decisions for more efficient control and eradication.

Keywords: molecular epidemiology, transboundary emerging diseases, virus dispersal.

INTRODUCTION

The rapid growth of global population along with the current demand for animal protein and the increasing animal trade have increased the spread of a broad range of transboundary animal diseases (TADs) [1, 2]. Clear examples of this phenomenon are the recent emergence of African Swine Fever in Asia, Avian Influenza or Contagious Bovine Pleuropneumonia and the return of Foot-and-mouth disease virus (FMDV) to Korea and other countries which successfully eliminated the virus for several years [3–7]. Understanding the tempo and mode of disease evolution allows to estimate the impact of external factors influencing these diseases and assess the evolutionary patterns followed over time, which can be better studied by considering the most recent advances in virus sequencing and phylogenetics [8–10].

Molecular phylogenetics has shown to be an accurate and highly impacting approach in the understanding of the spatiotemporal dynamics of infectious diseases, with the capacity to explain disease spread, virulence and invasion potential [11–20]. In the case of TADs, molecular phylogenetics has also proven to be a useful approach, providing accurate knowledge for the control of pathogens worldwide [21–24], however, it remains underused.

FMDV causes the most influential transboundary animal disease with historical worldwide circulation reported in domestic and wildlife reservoirs [25, 26]. FMD is a highly contagious disease caused by a small single-stranded RNA virus of the genus *Aphthovirus*, member of the family Picornaviridae [27] and classified into seven different serotypes; O, A, C, Asia1 and Southern African Territories (SATs) 1, 2 and 3 [25, 28–30] which severely affect the productivity of domesticated livestock, causing great economic losses [31–33]. The United States Department of Agriculture has estimated that the introduction of FMDV could result in losses between $15 to $100 billion [34–37]. One of the main reasons for this great impact is the wide variety of hosts known for FMDV (i.e., cattle, buffalo, swine, sheep, and deer), altogether it affects more than 70 species of cloven-hoofed animals [38]. FMDV is known to be transmitted locally and globally, often associated with infected animal products and human and animal movements [39, 40]. Transmission is also facilitated by airborne spread, direct animal contact with infected individuals or carcasses and translocation of contaminated staff, equipment, and machinery [41, 42].

Individual genes have been widely used to study the phylogenetic relationships among FMD serotypes [43–50], however, little has been done using whole genome sequences (WGS) [26, 51–53]. Nevertheless, these studies have been often based on a limited number of sequences (<200), or on phylogenetic methods that do not have the ability to accommodate uncertainty (i.e., Bayesian phylodynamic methods) [54]. Although these methods have been widely used, they present certain degree of evolutionary inaccuracy since in most cases (excluding Yoon et al (2011) and Omondi et al (2019)) the Bayesian phylogenetic and

78 phylodynamic methods were not considered. Thus, their inherent ability to accommodate
79 uncertainty, and therefore to assess the level of error of the predictions obtained, was often
80 neglected.

81 Several studies have explored the spatiotemporal evolutionary dynamics of FMDV in
82 different parts of the world, mainly focusing on the diffusion patterns across its endemic regions:
83 Asia and Africa [31, 48, 55–59] However, studies considering all serotypes are only available
84 within small geographic regions, and global studies only assessed some of the viral serotypes
85 [56, 60].

86 In this study, we investigated the spatiotemporal dynamics of FMDV by using Bayesian
87 phylodynamic analyses of comprehensive genetic, geographical and temporal data regarding
88 past FMDV occurrences. The objectives of this work were to reconstruct the global evolutionary
89 epidemiology of FMDV serotypes O, A, Asia1, and SATs, to make comparisons among the
90 global spatiotemporal spread of each FMDV serotype, identify ancestral countries and provide
91 inferences about the evolutionary patterns and the transmission between host species.

92

93 **MATERIALS AND METHODS**

94 **Data collection and curation**

95 We built a comprehensive genetic database comprising 249 publicly available whole genome
96 sequences from six FMDV serotypes (A, O, Asia1, SAT 1, SAT 2 and SAT 3), with collection
97 dates ranging from 1959 to 2017 (GenBank ID numbers in Supplementary material Table S1).
98 Serotype C was not included in this study due to data unavailability (only 3 sequences were
99 available). Our dataset gathers information from 43 countries and 4 continents obtained from
100 the Virus Pathogen Resource database, available at https://www.viprbrc.org (See Table S1). To
101 determine accurate phylogenetic relationships among FMDV reports, we combined the available
102 genetic information along with collection date, host species (i.e., *Bos taurus*= cattle, *Syncerus*
103 *caffer*= African buffalo, *Bubalus bubalis*= Water buffalo, *Sus scrofa domesticus*= swine, *Sus*

104 *scrofa*= boar, and *Ovis aries*= sheep) and location (discrete information at country level) as
105 metadata information. Any sample lacking one of these three characteristics was discarded.
106
107 **Discrete phylogeographical analysis**
108 Sequences were aligned using Mega X, available at www.megasoftware.net [61]. The
109 recombination detection program (RDP) v5.3 was used to search for evidence of recombination
110 within our dataset [62]. Each serotype was screened using five different methods (BootScan,
111 Chimaera, MaxChi, RDP, and SiScan). After removing all the duplicated sequences (i.e.,
112 representing the same outbreak), no evidence of recombinant sequences was observed in any
113 FMDV serotypes analyzed. To determine whether there was a sufficient temporal molecular
114 evolutionary signal of the FMDV sequences used for each serotype phylogeny, we used
115 TempEst v1.5 [63]. To calculate the *P*-values associated with the phylogenetic signal analysis,
116 we used the approach described by [64] based on 1,000 random permutations of the sequence
117 sampling dates [65]. The relationship found between root-to-tip divergence and sampling dates
118 (years) supported the use of molecular clock analysis in this study for all serotypes. Root-to-tip
119 regression results for each serotype are reported in Supplementary Table S2, all the results
120 supported a significant temporal signal (*P*-value<0.05). Phylogeographic history of FMDV
121 dispersal was recovered from the obtained spatiotemporal phylogenies for each serotype.
122 Phylogenetic trees were generated by a discrete phylogeography estimation by Bayesian
123 inference through Markov chain Monte Carlo (MCMC), implemented in BEAST v2.5.0 [66]. We
124 partitioned the coding genes into first+second and third codon positions and applied a separate
125 Hasegawa-Kishino-Yano (HKY+G; [67]) substitution model with gamma-distributed rate
126 heterogeneity among sites to each partition [68].
127 By using Nested Sampling Beast package v1.0.4 [69] we compared different molecular
128 clock models to find the one that showed the best fit for the data related to each serotype. The
129 marginal likelihood value supported the use of uncorrelated lognormal relaxed molecular clock

[70]. To infer the epidemic demographic histories of FMDV per each serotype we estimated the effective number of infections through time by using the Bayesian skyline plot approach [71]. All analyses were developed for 200 million generations, sampling every 10,000th generation and removing 10% as chain burn-in. All the Markov chain Monte Carlo analyses for each serotype were investigated using Tracer software v1.7 [72] to ensure adequate effective sample sizes (ESS) (above 200), which were obtained for all parameters. Final trees were summarized and visualized via Tree Annotator v. 2.3.0 and FigTree 1.4.3 respectively (included in BEAST v2.5.0) [66, 73].

To reconstruct the ancestral-state phylogeographic transmission across countries and hosts, we used the discrete-trait extension implemented in BEASTv2.5.0 [66]. In addition, to explore the most important historical dispersal routes for the spread FMDV across countries, as well as most probable host-species transition, we used a Bayesian stochastic search variable selection (BSSVS) [74]. Using BSSVS approach, we identified and eliminated the nonzero rates of change between each pair of discrete traits (countries and hosts species) based on its Bayes factor value obtained (lower than 3). To perform this analysis, a symmetric rate matrix was assumed. To infer the intensity of directional transitions (forward and backward) within a matrix of the discrete traits mentioned above, we used a Markov jumps approach. To interpret the Bayes factors, a value of <3, as mentioned above, is not significant (hardly worth mentioning), BF= 3.1-20 represents positive support, BF= 20.1-150 represents strong support, while >150.1 represents an overwhelming support [75].

Finally, we visualized the spatiotemporal viral diffusion of each serotype by using Spatial Phylogenetic Reconstruction of Evolutionary Dynamics using Data-Driven Documents (D3) SPREAD3 software [76] considering the whole transmission and also the most significant connections between localities following the Bayesian stochastic search variable selection (BSSVS) method, with each country used as a discrete variable with a cutoff BF > 3 [75]. In addition, we classified the viral spread of each serotype in two categories: local, if the

transmission occurs through neighboring countries, and long distance, if the dispersion jumps beyond adjacent neighboring countries.

RESULTS

The number of available sequences per country varied from 1 to 18 whole genome sequences (WGS). Our results showed that India, China, Uganda, Argentina, and Zimbabwe were the countries with the highest number of available genomes (Supplementary Table S3). Likewise, several countries have been historically affected by more than one serotype, particularly in Africa and Asia, where we observed that Uganda presented the highest virus diversity as it has been subjected to the spread of serotypes O, and all SATs (Supplementary Table S3, Supplementary Fig. S1).

Spatiotemporal dynamics of FMDV

Phylogeographic analyses highlighted great asymmetries in the tempo and mode of each serotype evolution (Fig. 1). SAT1 appeared to be the basal clade of the entire lineage, originating SAT2, SAT3 and serotype A, which later diversified into serotype Asia1, and O. Our analysis suggested O as the most recent, prolific and widespread lineage, with the highest number of sequences available worldwide. Serotype A and Asia1 appeared second and third in the number of available sequences, followed by all SAT serotypes. Maximum clade credibility phylogeny showed the monophyly of serotypes O, A, and Asia1 (each serotype shared a common ancestor), while SAT serotypes appeared to have multiple origins (Fig. 1).

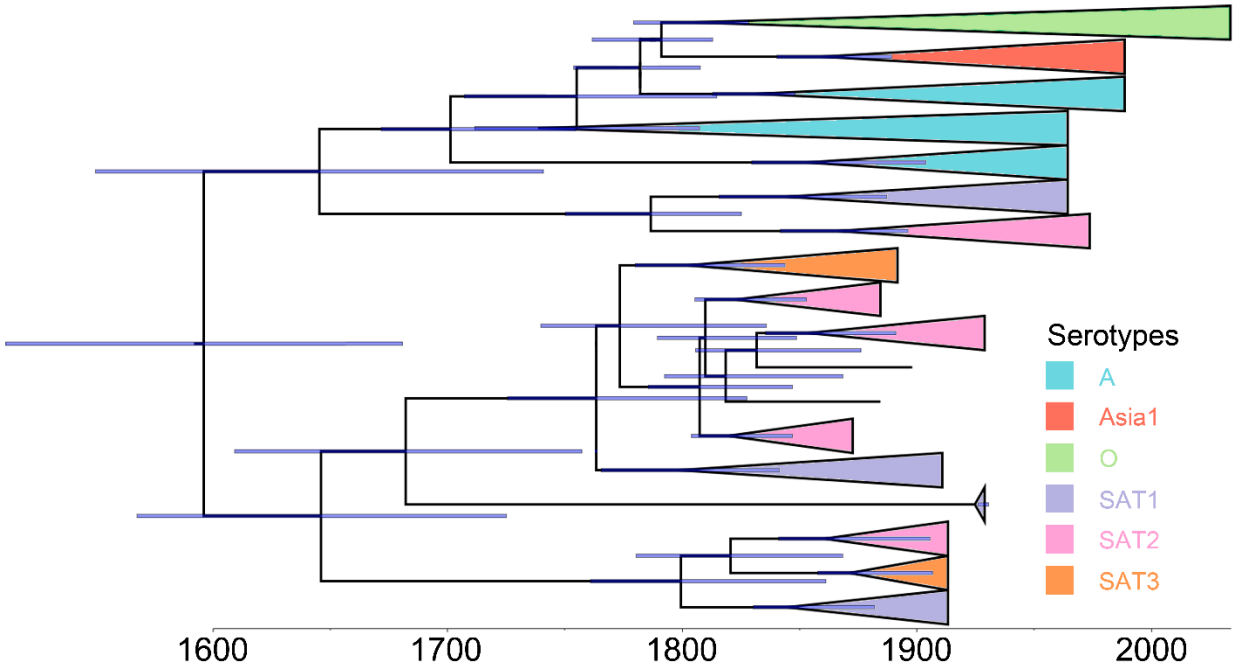

Fig. 1 Condensed phylogenetic tree showing the overall evolutionary history of FMDV representing the relationships between all serotypes. The tree is based on a maximum clade credibility phylogeny inferred from 249 whole genome sequences. Branch bars represent posterior probabilities of branching events ($P > 0.95$).

Spatiotemporal diffusion among serotypes

We investigated and compared the historical spreads of FMDV at serotype level, from the ones with local distribution (Asia1 and SATs) to the serotypes with widespread dispersal (O and A) (Sobrino et al., 2001; Fèvre et al., 2006; Di Nardo et al., 2011; Jamal and Belsham, 2013; Knight-Jones and Rushton, 2013; Brito et al., 2017).

Serotype O

We analyzed 97 WGS from serotype O, which comprises 39% of the global FMDV tree (Fig. 1). This serotype also presents the widest distribution of all serotypes, with records from 42 countries (Fig. 2). Based on our phylogeographic analysis, the most likely center of origin for

this serotype was Belgium (root state posterior probability [RSPP] = 0.27) from which it spread globally across long distances to several countries through Europe, Asia, Africa and South America. A remarkable aspect of this global spread is that most of it has occurred in less than 50 years (Fig. 3A) (see Supplementary Video S1 for detailed footage). These patterns have also appeared in our spatiotemporal diffusion map, which shows that the global distribution of this serotype is highly represented by long-range movements across countries and continents (Fig. 3A). Phylogenetic reconstruction identified clusters formed by different sub-lineages, where the most representative centers of dispersal events (geographic spread accompanied by diversification) for this serotype were Poland and the United Kingdom in Europe, China, Japan, and Indonesia in Asia, Egypt in Africa and Argentina in South America. Likewise, we observed that China, South Korea, and Turkey were also among the countries with the highest number of sequences (see Fig. 1A). In addition, BSSVS-BF results showed the most significant viral transmission routes for serotype O, where the most intense were represented from Turkey to Egypt, from Egypt to Indonesia and from Myanmar to Japan (BF>1038.7) (Fig. 3B).

Serotype O also showed the highest host diversity among all FMDV serotypes, which is represented by cattle (*Bos taurus*), swine (*Sus scrofa domesticus*), boar (*Sus scrofa*), sheep (*Ovis aries*), and the water buffalo (*Bubalus bubalis*), where the most representative were *B. taurus* (71% of the sequences) and *S. scrofa domesticus* (20%). *B. taurus* was not only the most important host for this serotype but also the most likely initial host of the ancestral lineages (RSPP= 0.95), followed by *S. scrofa domesticus* (RSPP= 0.03) and *O. aries* (RSPP= 0.032) respectively (Fig. 2). Bayes factor analysis showed that the most significant transmission routes occurred from *B. taurus* to *S. scrofa domesticus* (BF= 635.3), followed by from *B. taurus* to *O. aries* (BF=73.6), and in a minor scale, from *S. scrofa domesticus* to *B. taurus* (BF= 9.7), as well as from *B. taurus* to *B. bubalis* (BF=9.1) (Fig. 3C).

The Bayesian skyline plot (BSP) was used to describe the observed changes in genetic diversity (population size) through time, showing a steady pattern in this serotype, with a sharp

219 decrease in its effective population size occurred ~2000, which returned to previous rates years
220 later (Fig. S2).

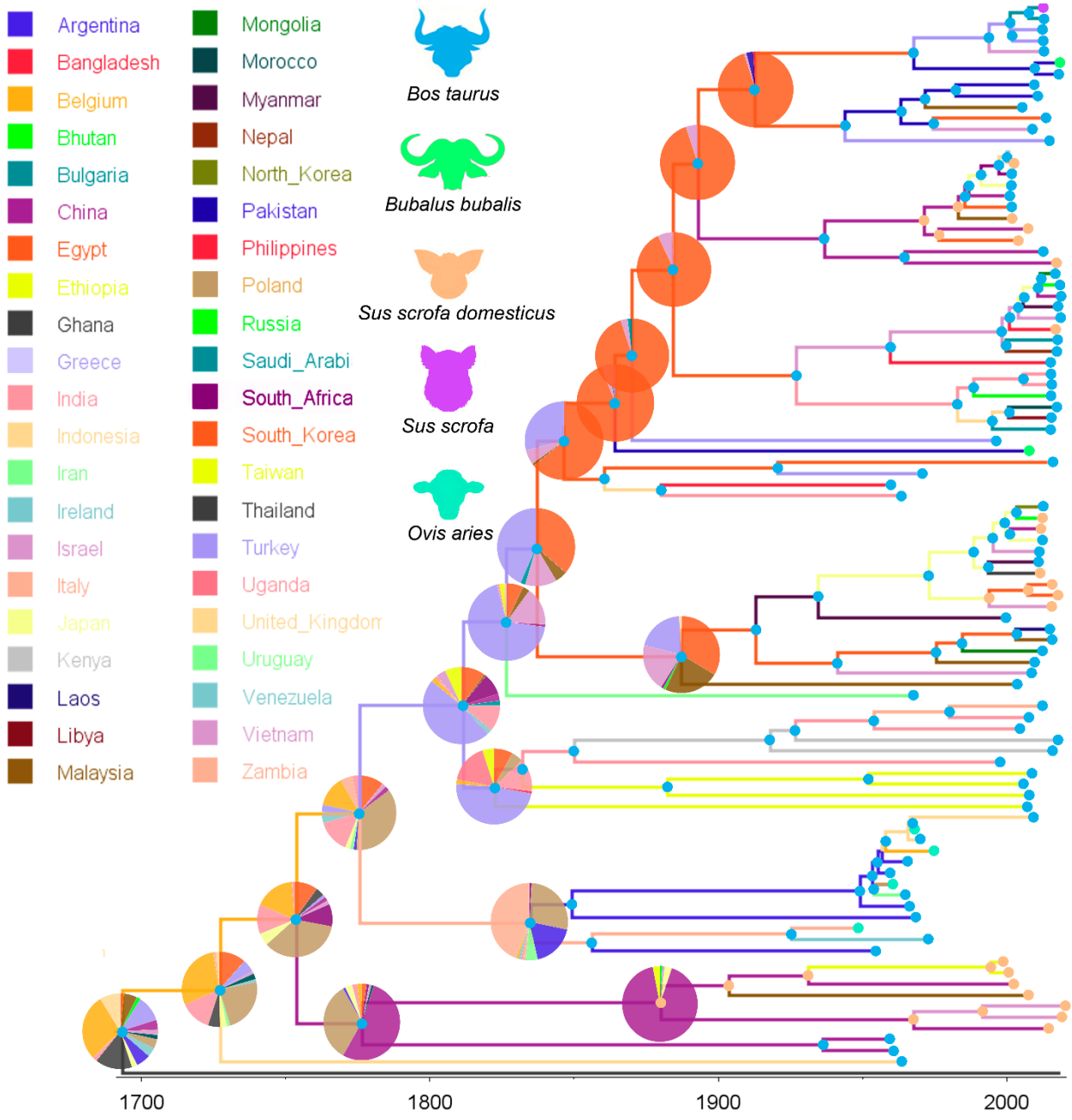

221

222 **Fig. 2** Dispersal history of FMDV lineages of Serotype O, as inferred by discrete
223 phylogeographic analysis. Maximum clade credibility phylogeny colored according to the
224 countries of origin. Branch bars represent posterior probabilities of branching events (P > 0.95).
225 Colored dots at the end of the branches represent the host species (*Bos taurus*= cattle, *Sus*

scrofa domesticus= swine, *Ovis aries*= sheep, *Bubalus bubalis*= water buffalo, and *Sus scrofa*= *boar*). The probabilities of ancestral states (inferred from the Bayesian discrete trait analysis) are shown in pie charts at each node, while circles on each branch and tips represent the most likely hosts.

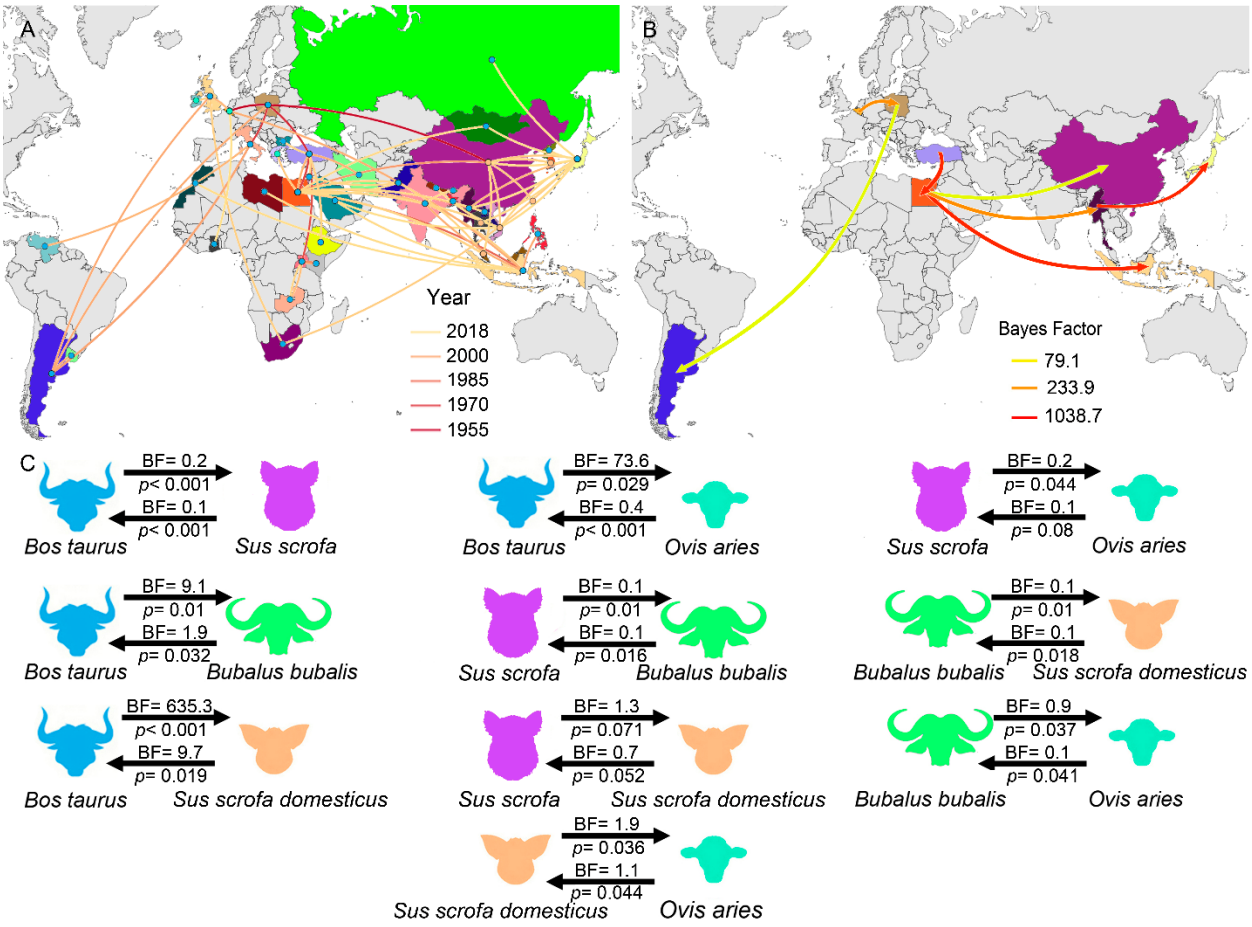

Fig. 3 (A) Reconstructed spatiotemporal diffusion of FMDV serotype O spread, the color of the branches represents the age of the internal nodes, where darker red colors represent older spread events. (B) Representation of the most significant location transitions events for FMDV serotype O spread based on only the rates supported by a BF greater than 3 are indicated, where the color of the branches represent the relative strength by which the rates are supported. (C) Transmission rates between hosts (*Bos taurus*= cattle, *Sus scrofa domesticus*= swine, *Ovis aries*= sheep, *Bubalus bubalis*= water buffalo, and *Sus scrofa*= *boar*). based on

238 BSSVS-BF values are represented on the top of the black arrows, while the root state posterior
239 probability for the host-species transition are given on its bottom.
240
241 **Serotype A**
242 Phylogeographic relationships obtained for serotype A indicated India as its most likely center of
243 origin (RSPP= 0.28, Fig. 4). Besides, several centers of diversification have been identified for
244 this serotype, where the most important have been India and Malaysia in Asia, Netherlands and
245 Germany in Europe, Chad in Africa and Brazil in South America (Fig. 4). Our phylogeographic
246 analysis also highlighted the importance of Brazil as a center of origin for a wide variety of
247 European and South American lineages (Fig. 4). As in serotype O, we observed that long-
248 distance dispersal events were the most representative of the spatiotemporal dynamics of this
249 serotype, evidencing a global distribution, with records from 33 countries (Fig. 5B), which
250 represents 33% of the total FMDV sequences.
251 BSSVS-BF analysis evidenced that the most significant transmission routes for this
252 serotype come from India. Bayesian Factor analysis describing the most important viral
253 transmission routes highlighted the importance of India in different directions, mainly to
254 Netherlands (BF= 173.2), to Chad (BF= 162.9), and to Malaysia (BF= 28.3). Likewise, some
255 European, such as Germany appeared to be important for the spread of this serotype into South
256 America (BF=81.6, Fig. 5B).
257 The host species that showed highest number of serotype A sequences comes from *B.*
258 *taurus* (82%), followed by *O. aries* (10%), *S. scrofa domesticus* (6%), and *B. bubalis* (2%)
259 (Supplementary Table S1). Thus, the most important host behind the origin of the analyzed
260 sequences of serotype A was *B. taurus* (RSPP= 0.98, Fig. 4). Furthermore, Bayes factor
261 analysis indicated that the most significant transmission routes for the spread of this serotype
262 occurred from *B. taurus* to all the other host. In order of significance, we can observe: to *S.*
263 *scrofa domesticus* (BF= 1256.8), to *B. bubalis* (BF= 628.5), and to *O. aries* (BF= 74.1, Fig. 5C).

264 The BSP for this serotype showed a constant lineage diversity with a slight increase in
265 1980. The biggest variations between the years 2000 -2017, showed a sharp decrease followed
266 by a rapid increase in lineage diversity that was maintained until 2010 when these values mostly
267 returned to the original values (Fig. S2).

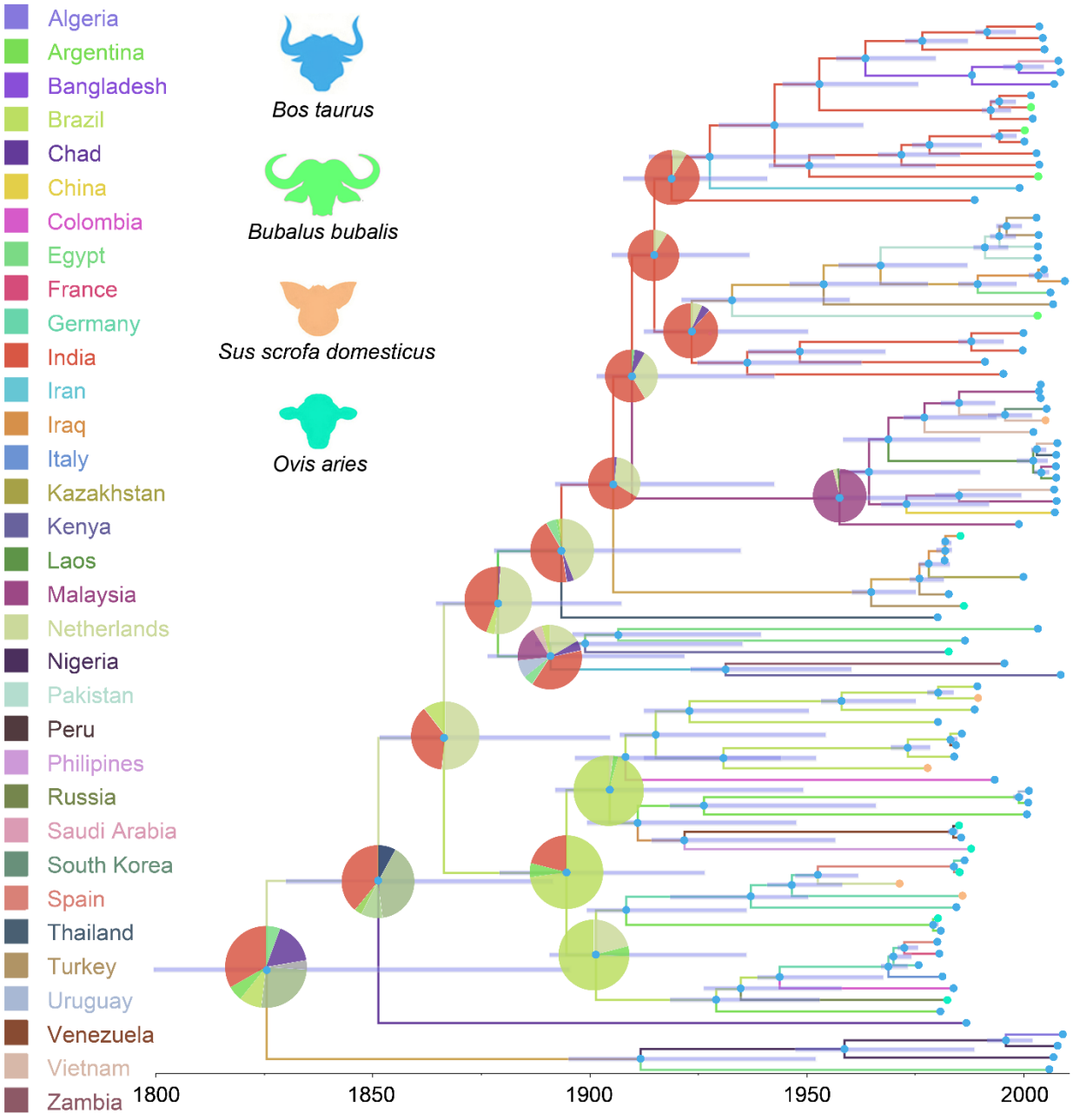

268

269 **Fig. 4** Dispersal history of FMDV lineages of Serotype A, as inferred by discrete
270 phylogeographic analysis. Maximum clade credibility phylogeny colored according to the

271 countries of origin. Branch bars represent posterior probabilities of branching events (P > 0.95).
272 Colored dots at the end of the branches represent the host species (*Bos taurus*= cattle, *Sus*
273 *scrofa domesticus*= swine, *Ovis aries*= sheep, and *Bubalus bubalis*= water buffalo. The
274 probabilities of ancestral states (inferred from the Bayesian discrete trait analysis) are shown in
275 pie charts at each node, while circles on each branch and tips represent the most likely hosts.
276

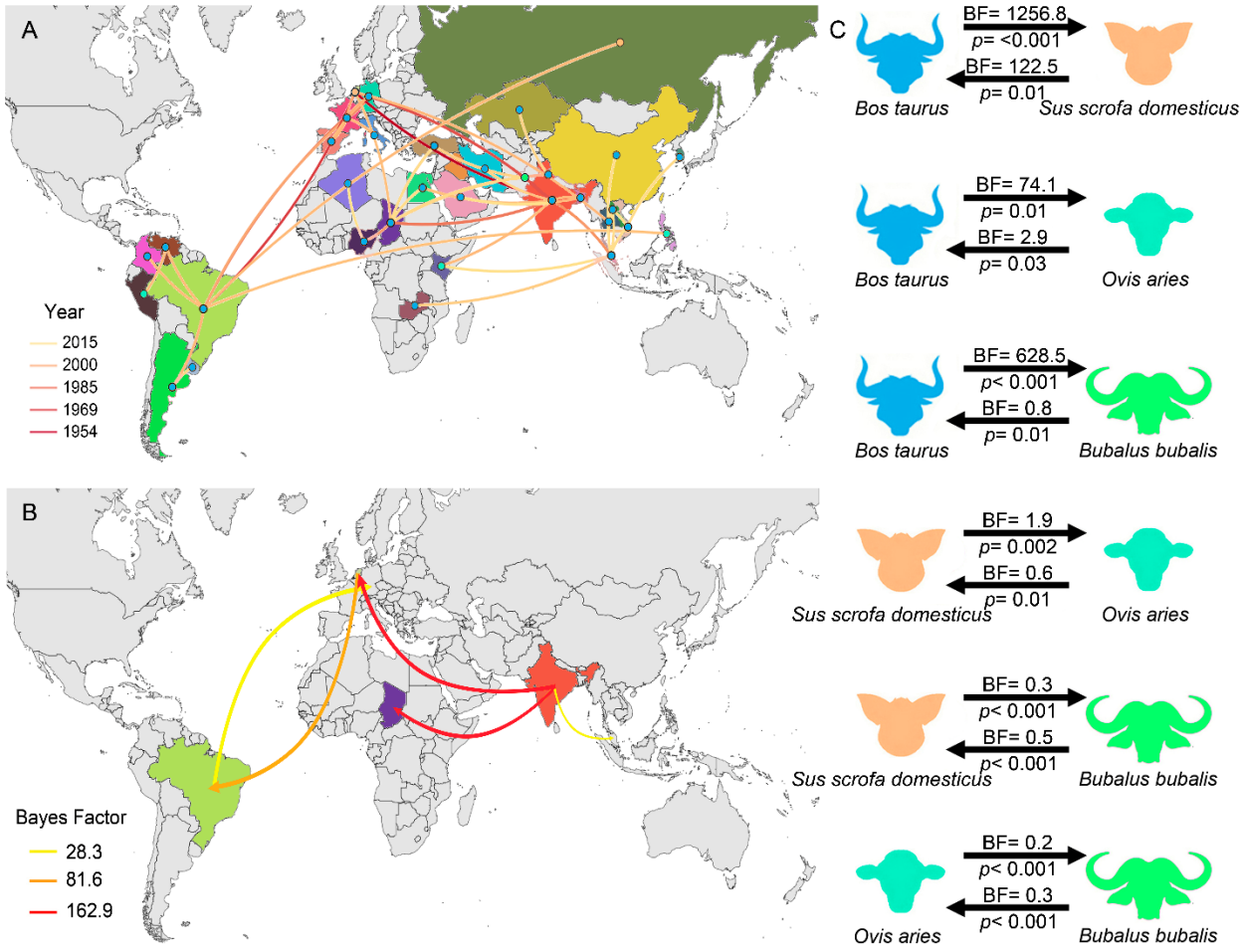

277

278 **Fig. 5** (A) Reconstructed spatiotemporal diffusion of FMDV serotype A spread, the color of the
279 branches represents the age of the internal nodes, where darker red colors represent older
280 spread events. (B) Representation of the most significant location transitions events for FMDV
281 serotype A spread based on only the rates supported by a BF greater than 3 are indicated,
282 where the color of the branches represent the relative strength by which the rates are

283 supported. (C) Transmission rates between hosts (*Bos taurus*= cattle, *Sus scrofa domesticus*=
284 swine, *Ovis aries*= sheep, and *Bubalus bubalis*= water buffalo) based on BSSVS-BF values are
285 represented on the top of the black arrows, while the root state posterior probability for the host-
286 species transition are given on its bottom.
287
288 **Serotype Asia1**
289 This serotypes represented 12% of the entire FMDV sequences. Similarly to serotype A,
290 phylogeographic analyses indicated India as the most likely origin of this serotype (RSPP=
291 0.34), from which it diverged in all directions (Fig. 6, Supplementary Video S3). The
292 phylogenetic relationships seen in this serotype show a clear disparity between the lineages
293 found in countries from western Asia (i.e., Israel, Lebanon, Afghanistan, and Turkey) and
294 eastern Asia (i.e., China, Mongolia, Malaysia, and Vietnam) (Fig. 7A). Phylodynamic analysis
295 shows that the most important centers of diversification for this serotype are India, China,
296 Pakistan and Vietnam (Fig. 7A). BSSVS-BF analysis showed similar results as the observed in
297 serotype A, where the most significant transmission routes are related to India. In order of
298 intensity, the most important routes are the ones from India to China (BF= 182.8) and from India
299 to Vietnam (BF= 61.5) (Fig. 7B).
300 In relation to the number of available sequences, the most representative hosts for this
301 serotype were *B. taurus* (66% of the sequences), followed by *S. scrofa* (14%, exclusively in
302 China), *Bubalus bubalis* (6%, observed in India, Vietnam, and China) and *Ovis aries* (~3%,
303 observed only in China). Phylogenetic analysis showed that the hosts responsible for the spread
304 of this serotype were *B. taurus* (RSPP= 0.98), followed by *S. scrofa* (RSPP= 0.2). In addition,
305 Bayes factor analysis indicated that the most strongly supported transmission routes for the
306 spread of this serotype occurred from *B. taurus* to *B. bubalis* (BF= 1405.6), followed by from *B.*
307 *taurus* to *S. scrofa* (BF= 401.3), and from *B. taurus* to *O. aries* (BF= 134.1) (Fig. 7C).

308 Phylodynamic patterns of serotype Asia1 spread through BSP approach showed a
309 constant lineage diversity over time, with a very slight variation around the year 2000 (Fig. S2).
310

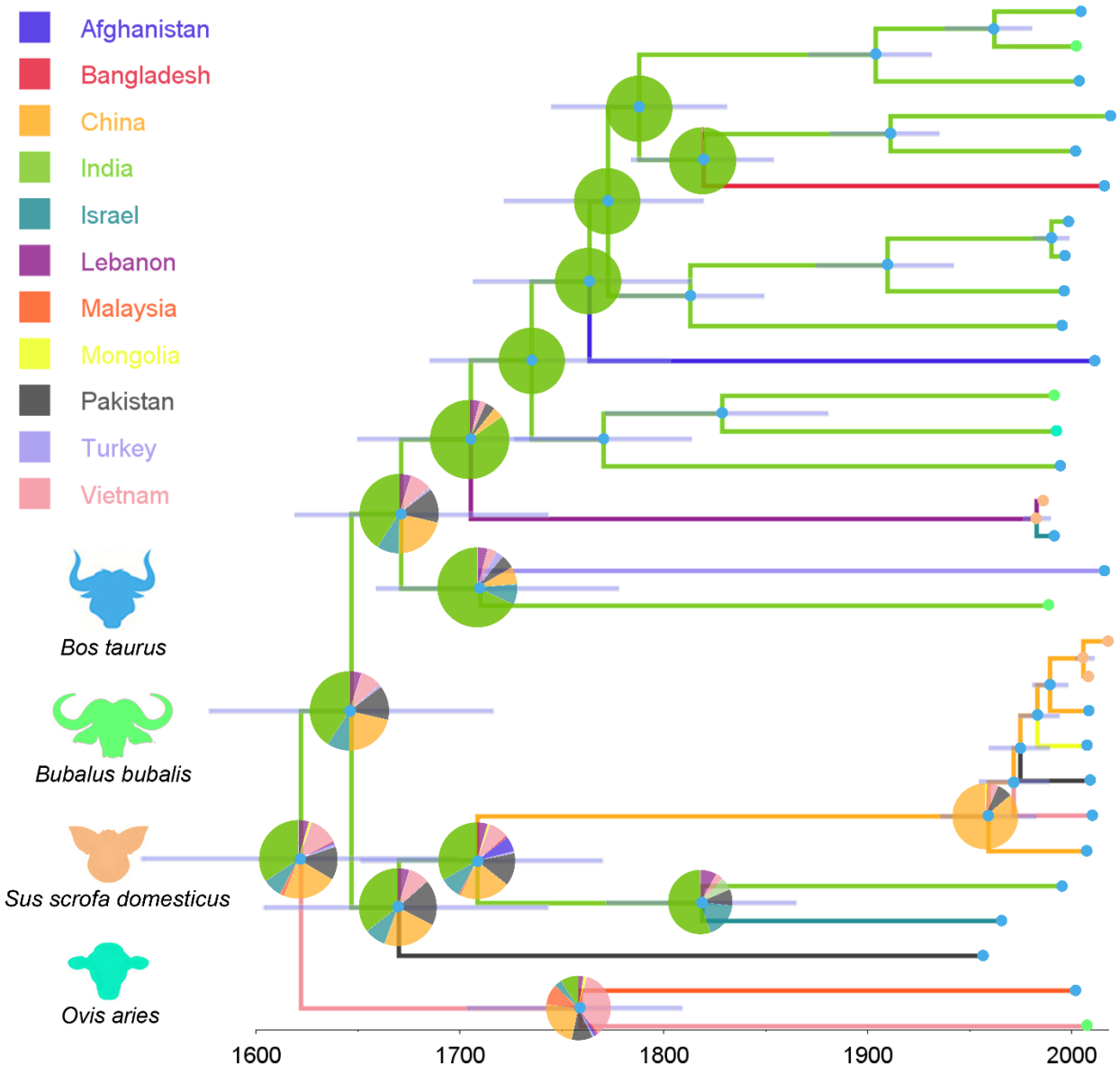

311

312 **Fig. 6** Dispersal history of FMDV lineages of Serotype Asia1, as inferred by discrete
313 phylogeographic analysis. Maximum clade credibility phylogeny colored according to the
314 countries of origin. Branch bars represent posterior probabilities of branching events (P > 0.95).
315 Colored dots at the end of the branches represent the host species (*Bos taurus*= cattle, *Sus*

316 *scrofa domesticus*= swine, *Ovis aries*= sheep, and *Bubalus bubalis*= water buffalo. The
317 probabilities of ancestral states (inferred from the Bayesian discrete trait analysis) are shown in
318 pie charts at each node, while circles on each branch and tips represent the most likely hosts.
319

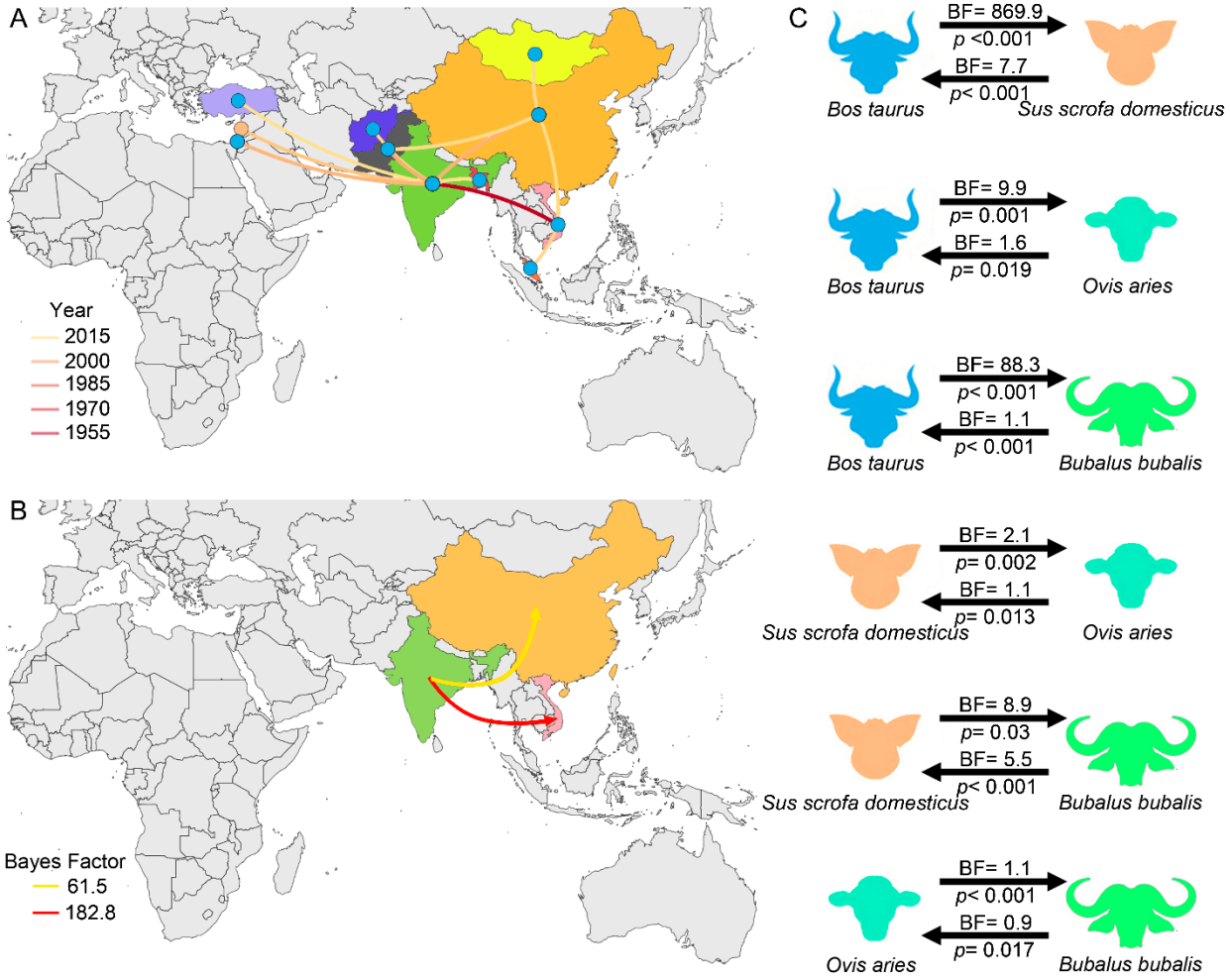

320

321 **Fig. 7** (A) Reconstructed spatiotemporal diffusion of FMDV serotype Asia1 spread, the color of
322 the branches represents the age of the internal nodes, where darker red colors represent older
323 spread events. (B) Representation of the most significant location transitions events for FMDV
324 serotype Asia1 spread based on only the rates supported by a BF greater than 3 are indicated,
325 where the color of the branches represent the relative strength by which the rates are
326 supported. (C) Transmission rates between hosts (*Bos taurus*= cattle, *Sus scrofa domesticus*=

swine, *Ovis aries*= sheep, and *Bubalus bubalis*= water buffalo) based on BSSVS-BF values are represented on the top of the black arrows, while the root state posterior probability for the host-species transition are given on its bottom.

Serotype SAT1

The phylogeographic patterns of SAT1 exposed Uganda as its most likely country of origin (RSPP= 0.45), from where it spread to Namibia, Nigeria, and Chad (Fig. 8). The phylogenetic relationships identified three main clusters, one of them represented by the ancestor of the lineages found in Uganda and Chad, other by the lineages located in the countries that are part of the southern area of spread (i.e., Botswana, Mozambique, Namibia, South Africa and Tanzania), and the last cluster represented by the lineages found in Nigeria, which also presented the sub-lineage with the most recent appearance. Contrary to the previous serotypes, SAT1 did not present a clear source (country) of dispersal events, although its spread was mostly concentrated on Eastern Africa (Fig. 9A). Our results showed that the highest proportion of its dispersal events occurred across long distance countries (representing 63% of the cases, See Supplementary Video S4 for detailed footage). The most significant dispersal routes were strongly related to Uganda, which in order of intensity, were seen to happen from Uganda to Nigeria (BF= 35.2), which seemed the most significant, followed by the transition from Kenya to Tanzania (BF= 26.5) (Fig. 9B).

The host species associated with the dispersal of this serotype were *Bos taurus* and *Syncerus caffer* (Fig. 8). *B. taurus*, with the majority of the number of sequences (58.3%), is mostly distributed in the north and central Africa, while *S. caffer* (41.7%, appeared as the most common host species in the southern countries (i.e., Namibia, Botswana, and South Africa). Phylogenetic analysis suggested *B. taurus* as the most important host species for the origin of this serotype (RSPP= 0.98). Strongly supported transmission routes were inferred from *B.*

352 *taurus to S. caffer* (BF= 1233.3). However, the reverse transmission was not significant (BF<3)
353 (Fig. 8).

354 Intriguingly, SAT1 BSP showed the most variable lineage diversity between all SATs,
355 with an early increased in 1860 that was maintained until 1970, where this diversity increased
356 again, reaching the values observed today (Fig. S2).

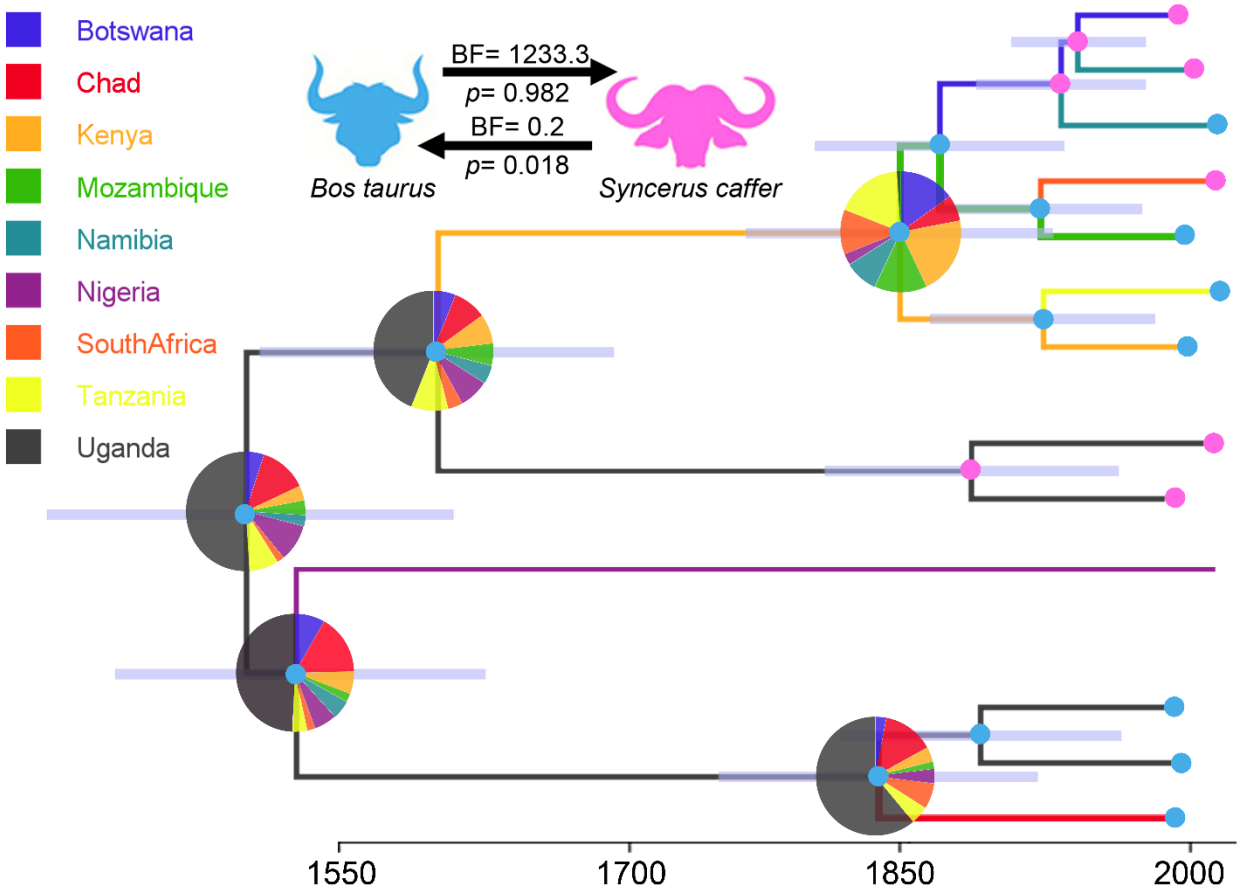

357

358 **Fig. 8** Dispersal history of FMDV lineages of Serotype SAT1, as inferred by discrete
359 phylogeographic analysis. Maximum clade credibility phylogeny colored according to the
360 countries of origin. Branch bars represent posterior probabilities of branching events (P > 0.95).
361 Colored dots at the end of the branches represent the host species (*Bos taurus*= cattle, and
362 *Syncerus caffer*= African buffalo. The probabilities of ancestral states (inferred from the
363 Bayesian discrete trait analysis) are shown in pie charts at each node, while circles on each
364 branch and tips represent the most likely hosts. Transmission rates between hosts (BSSVS-BF

365 values) are represented on the top of the black arrows, while the root state posterior probability
366 for the host-species transition are given on its bottom.
367

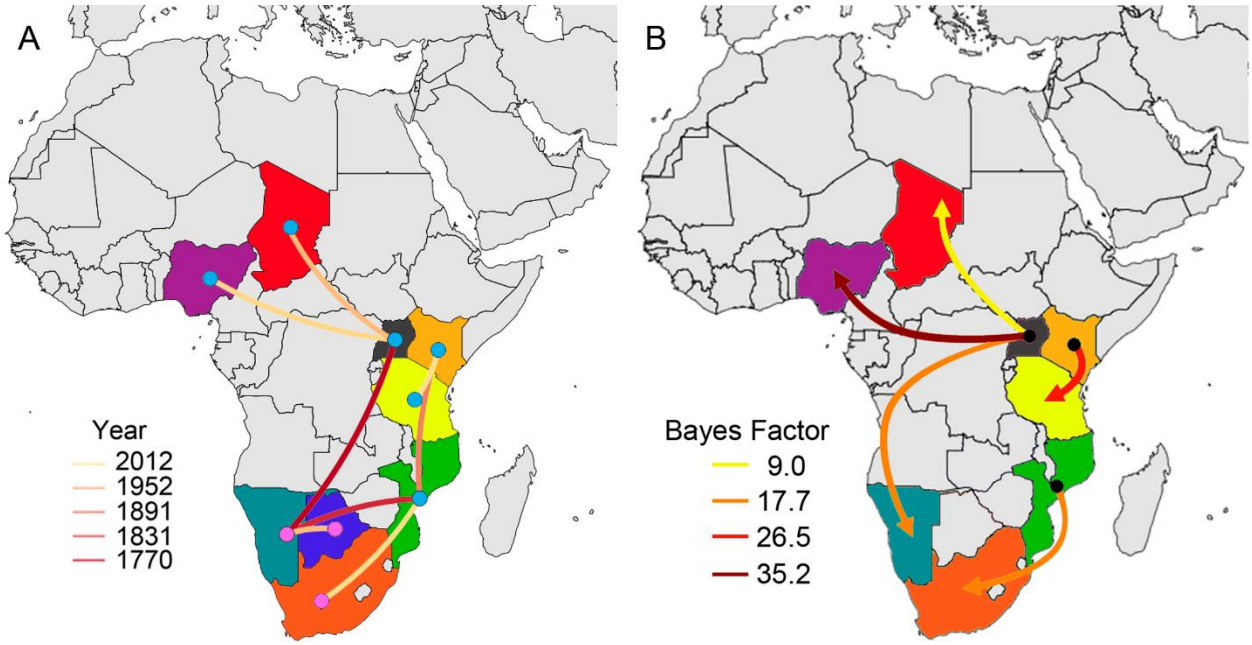

368

369 **Fig. 9** (A) Reconstructed spatiotemporal diffusion of FMDV serotype SAT1 spread, the color of
370 the branches represents the age of the internal nodes, where darker red colors represent older
371 spread events. (B) Representation of the most significant location transitions events for FMDV
372 serotype SAT1 spread based on only the rates supported by a BF greater than 3 are indicated,
373 where the color of the branches represent the relative strength by which the rates are
374 supported.
375

376 **Serotype SAT2**

377 Phylogeographic analyses for SAT2 indicated Uganda as the most likely origin of the serotype
378 (RSPP= 0.51), from which it spread to Botswana and The Gaza Strip later on time (Fig. 10).
379 Later, from Botswana, this serotype expanded its distribution to Ethiopia, Zimbabwe, and
380 Zambia, continuing spreading to surrounding countries also on the Eastern region of Africa (see
381 Supplementary Video S5 for detailed footage). Phylogenetic analysis identified two main sub-

382 lineages, one found between Uganda and Gaza Strip and the second cluster formed by the
383 lineages found in countries distributed in southeastern Africa (Fig. 10). Likewise, our results also
384 evidenced that serotype SAT2 spread is mostly characterized by a higher proportion of long-
385 distance movements (57%) over local dispersal events (Fig. 11A). Our phylodynamic model
386 suggested that the strongest geographic transition routes occurred from Uganda to Gaza Strip
387 (BF= 34.6), and from Botswana to Zambia (BF= 23.2) (Fig. 11B).
388 *B. taurus and S. caffer* were also the main host associated with SAT2 sequences, but in
389 this case, *S. caffer* was the most representative (53.9%), over *B. taurus* (46.1%). However, *B.*
390 *taurus* appeared in most of the reported locations (except in South Africa), while *S. caffer* was
391 only described in Uganda, Botswana and South Africa. As observed in SAT1, phylogenetic
392 analysis showed a higher influence of *B. taurus* as the host of the ancestral lineages of this
393 serotype (RSPP= 0.63) (Fig. 10). Transmission dynamics between host species suggested that
394 transmission from *B. taurus to S. caffer* was the most important (BF= 911.4), while transmission
395 from *S. caffer* to *B. taurus* was not significant (BF<3) (Fig. 7D). Finally, BSP showed no variation
396 in the lineage diversity found over time (Fig. S2).
397

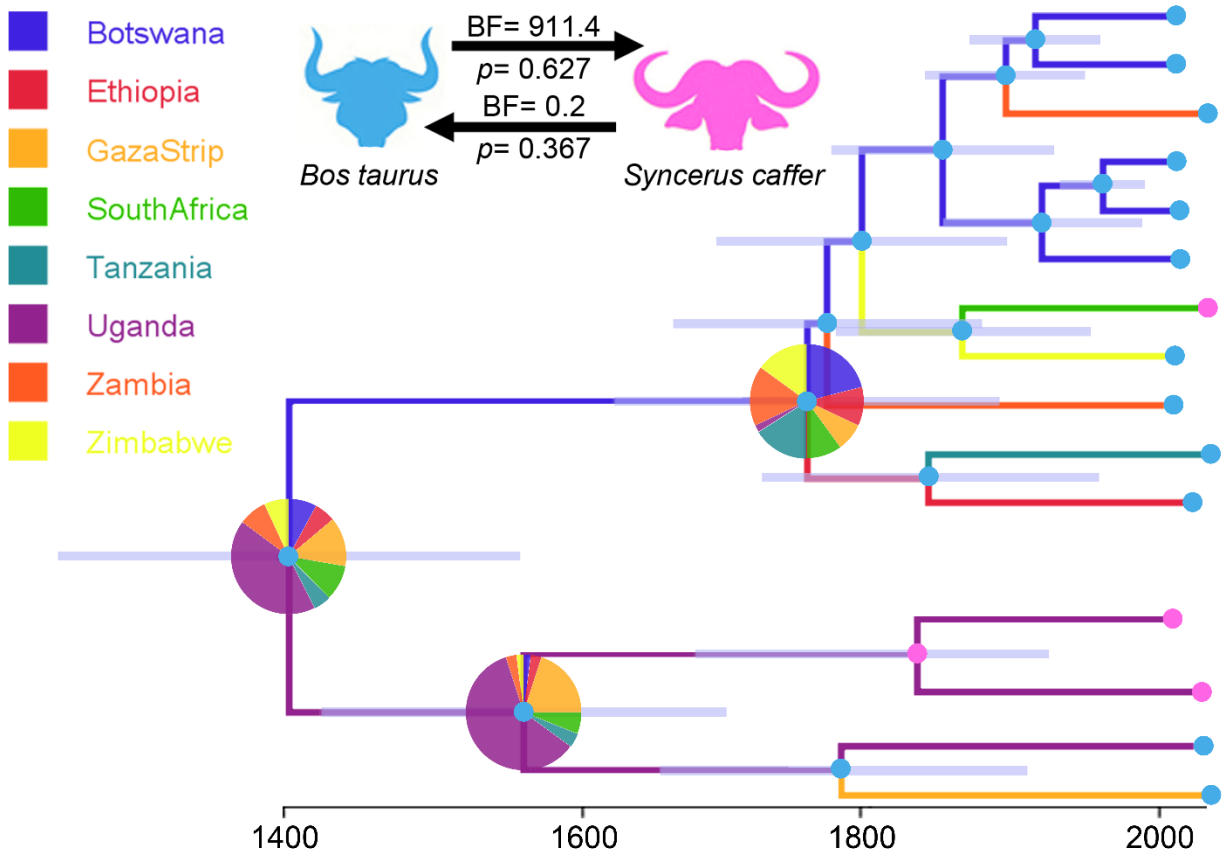

Fig. 10 Dispersal history of FMDV lineages of Serotype SAT2, as inferred by discrete phylogeographic analysis. Maximum clade credibility phylogeny colored according to the countries of origin. Branch bars represent posterior probabilities of branching events (P > 0.95). Colored dots at the end of the branches represent the host species (*Bos taurus*= cattle, and *Syncerus caffer*= African buffalo. The probabilities of ancestral states (inferred from the Bayesian discrete trait analysis) are shown in pie charts at each node, while circles on each branch and tips represent the most likely hosts. Transmission rates between hosts (BSSVS-BF values) are represented on the top of the black arrows, while the root state posterior probability for the host-species transition are given on its bottom.

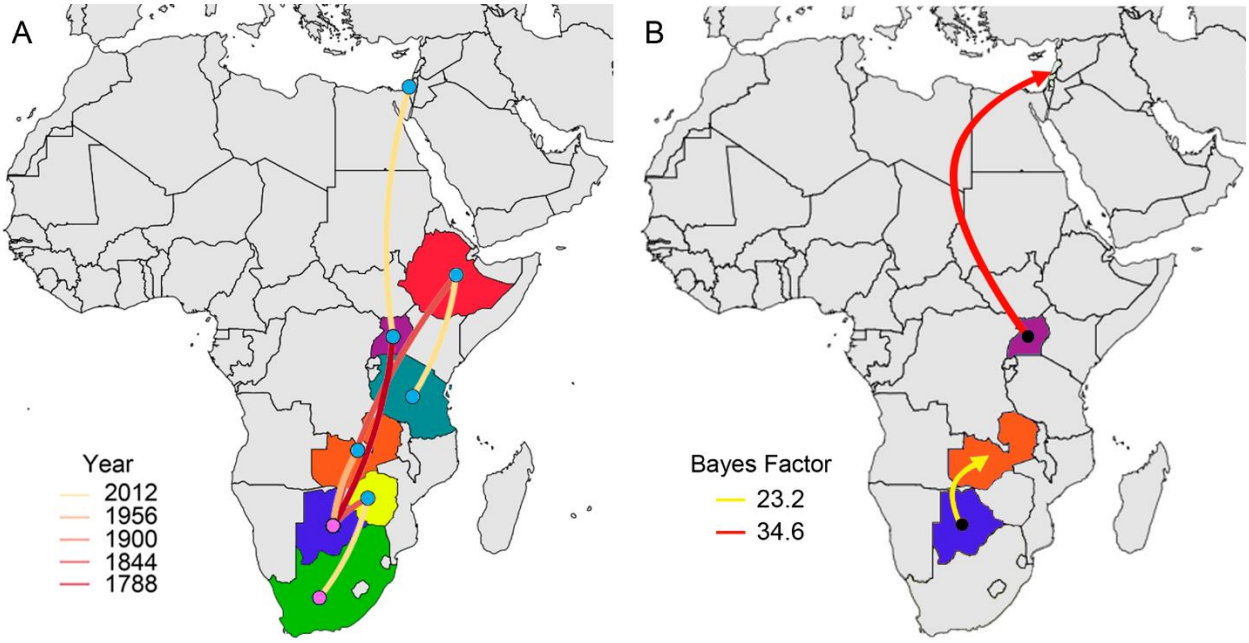

Fig. 11 (A) Reconstructed spatiotemporal diffusion of FMDV serotype SAT2 spread, the color of the branches represents the age of the internal nodes, where darker red colors represent older spread events. (B) Representation of the most significant location transitions events for FMDV serotype SAT2 spread based on only the rates supported by a BF greater than 3 are indicated, where the color of the branches represent the relative strength by which the rates are supported.

Serotype SAT3

Similar to the previous SAT serotypes, SAT3 also had its ancestral origin in Uganda (RSPP= 0.49), from where it traveled to Zimbabwe and then spread to its neighboring countries (Fig. 12, see Supplementary Video S6). Phylogenetic analyses identified two main sub-lineages, one of them found in Uganda and the second (and most diverse), present in the countries that are part of southern Africa (i.e., Botswana, South Africa, Zambia, and Zimbabwe). Phylogeographic reconstruction reflected the importance of Zimbabwe for the spread of this serotype, being this country the most common center of origin for the diffusion of the disease to Zambia, Botswana and most recently to South Africa. Contrary to all the other serotypes (except for Asia1),

425 spatiotemporal dynamics of serotype SAT3 showed that its spread has been dominated by local
426 events (75%, Fig. 13A). Based on BSSVS-BF results, the most significant viral transmission
427 routes for serotype SAT3 were represented by the dispersion from Zimbabwe to Botswana (BF=
428 15.9) and from Zimbabwe to South Africa (BF= 12.1) (Fig. 13B).
429 *B. taurus and S. caffer* were also the main hosts reported for SAT3, appearing both in a
430 similar proportion (*B. taurus*= 62.5%, and *S. caffer*= 37.5%). Similarly to all the serotypes above
431 mentioned, cattle was the likely ancestral host species for this serotype (RSPP= 0.94).
432 Furthermore, we found that most significant transmission routes for its spread occurred from *B.*
433 *taurus to S. caffer* (BF= 792.9), while the transmission in the opposite direction was not
434 significant (Fig. 12).
435 Like in the case of SAT2, the BSP obtained for this serotype showed no variation in the
436 lineage diversity over time (Fig. S2).
437

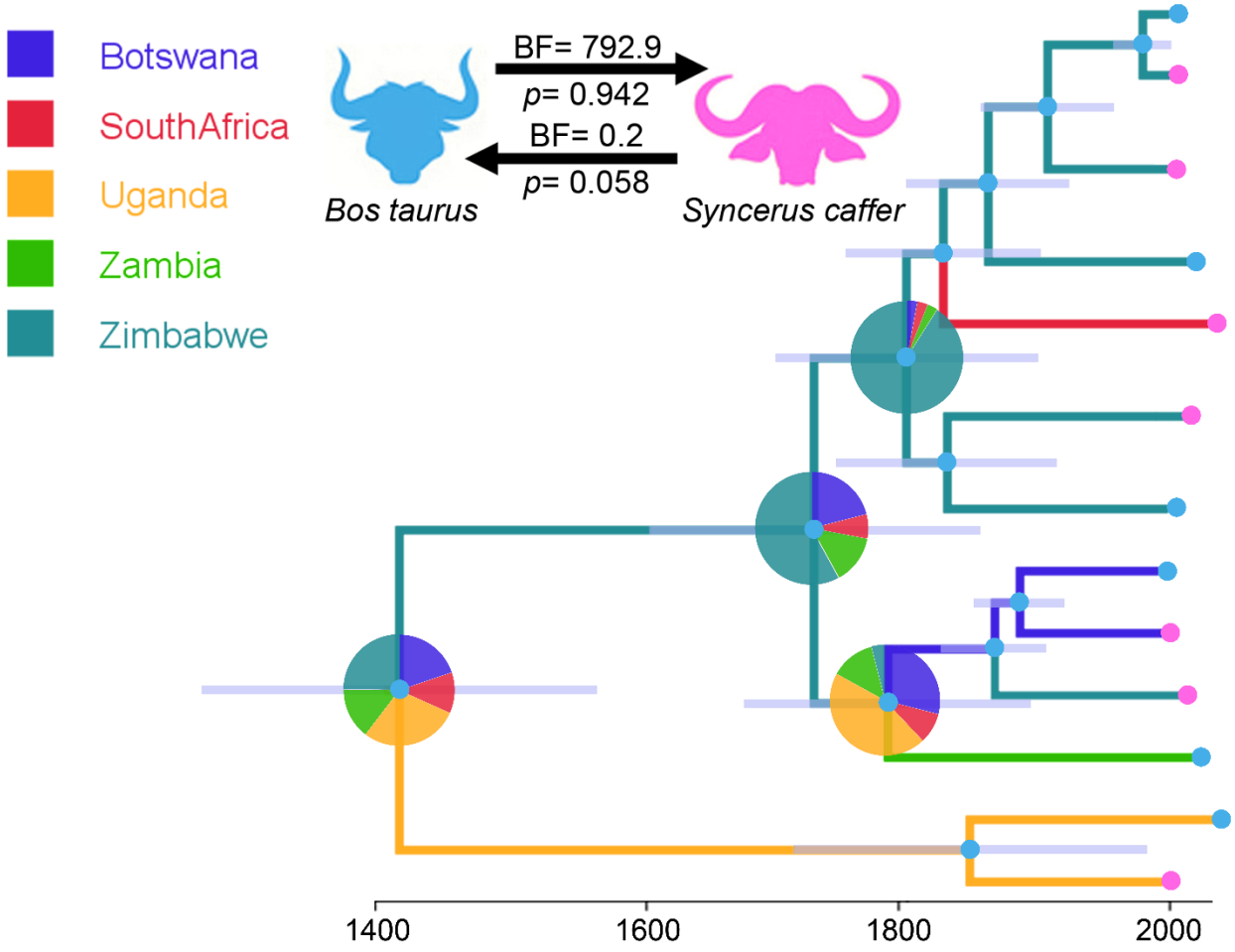

Fig. 12 Dispersal history of FMDV lineages of Serotype SAT3, as inferred by discrete phylogeographic analysis. Maximum clade credibility phylogeny colored according to the countries of origin. Branch bars represent posterior probabilities of branching events (P > 0.95). Colored dots at the end of the branches represent the host species (*Bos taurus*= cattle, and *Syncerus caffer*= African buffalo. The probabilities of ancestral states (inferred from the Bayesian discrete trait analysis) are shown in pie charts at each node, while circles on each branch and tips represent the most likely hosts. Transmission rates between hosts (BSSVS-BF values) are represented on the top of the black arrows, while the root state posterior probability for the host-species transition are given on its bottom.

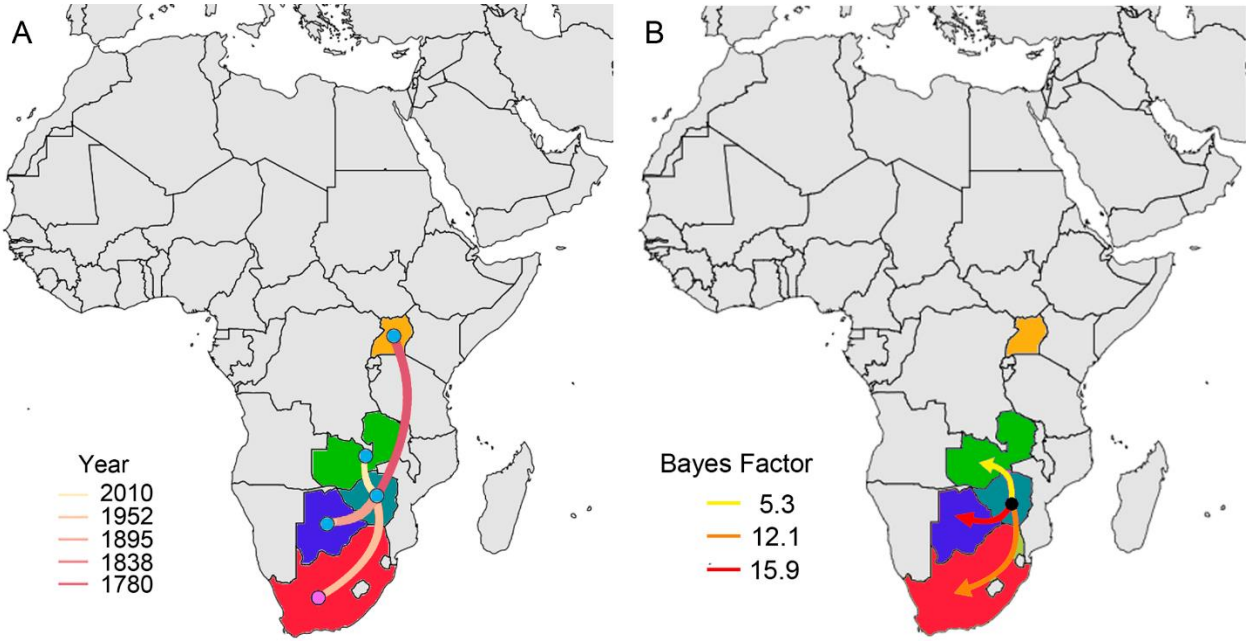

Fig. 13 (A) Reconstructed spatiotemporal diffusion of FMDV serotype SAT3 spread, the color of the branches represents the age of the internal nodes, where darker red colors represent older spread events. (B) Representation of the most significant location transitions events for FMDV serotype SAT3 spread based on only the rates supported by a BF greater than 3 are indicated, where the color of the branches represent the relative strength by which the rates are supported.

DISCUSSION

This study revealed new insights about the evolutionary dynamics of the FMDV's global transmission dynamics at serotype level. The most likely country of origin for each serotype was identified, along with its historical spread characteristics, and divergence patterns across its historical dispersal. Finally, we assessed the impact of each host interaction in the spread of FMDV, providing a comprehensive characterization of transmission dynamics between host species.

Phylogeographic patterns of FMDV spread

Global patterns of FMDV spread were considerably asymmetric in its spatiotemporal arrangement, showing important variation among all serotypes, as previously observed by Yoon et al., (2011) and Brito et al., (2015). On the other hand, our results yielded discrepancies regarding the phylogenetic relationships of FMDV serotypes due to the disagreements observed in the cladistic characterization of FMDV serotypes (monophyletic or polyphyletic origin) [52]. Lewis-Rogers et al. (2008) and Yoon et al. (2011) suggested that O, A, Asia1, C, and SAT3 were monophyletic, while SAT1 and SAT2 serotypes were polyphyletic. However, our results indicated the presence of only three monophyletic serotypes (O, A, and Asia1), whilst all SAT serotypes appeared to have multiple ancestral origins which can be related to multiple points of independent introduction of the virus.

Serotypes with global distribution (O and A)

Serotype O has shown a remarkable widespread distribution across the globe. In half of a century, this serotype reached almost all continents, causing dramatic economic losses [58, 77, 78]. Root state posterior probability analysis inferred Belgium as the most likely center of origin for this serotype, which, as a result of being responsible for the majority of outbreaks worldwide [79], we can observe multiple centers of diversification in most of the continents. Our phylogeographic analysis showed that this spread has been characterized by lineage dispersal events between distant regions (i.e. to regions not sharing international dry borders with the origin country), instead of dispersal events between neighboring countries, which may be one of the keys for its successful global spread. Bayesian skyline plot showed a severe decline in the genetic diversity around early 21th century, this interesting pattern also observed by Yoon et al., (2011). This decline and recover in the effective population size could be directly related to the increase in the FMDV outbreaks that occurred worldwide, which was followed by an intensive control and prevention strategies. The intense wave of outbreaks occurred during that period worldwide included countries such as, Argentina (Perez et al., 2004; Perez et al., 2004), the

492 United Kingdom [82, 83], Brazil [84], India [85], and Taiwan [86, 87]. As we observed in our
493 phylogeographic visualization, there is strong evidence that most of these outbreaks were
494 strongly interconnected [25, 88–90], evidencing local and long-distance spread of serotype.
495 One of the reasons for the success of the evolutionary diversification of this serotype
496 may also be related to the diversity of hosts that it affects, which is the highest among all
497 serotypes. Globally, *B. taurus* represented the most important host species for the spread of
498 serotype O, while *S. scrofa* was mostly related to the spread of this serotype in southeastern
499 Asia. Thus, phylodynamic analysis suggested that viral transition rate between these two
500 livestock was the strongest reported between all the reported hosts.
501 Following the pandemic patterns showed by serotype O, the next large-scale potential of
502 diffusion was exhibited by serotype A. Phylogeographic analysis suggested India as the most
503 likely center of origin of the current circulating serotype A strains. Supporting previous studies
504 [26, 60], we observed that India was also a key source of dispersal events for this serotype
505 since most of the current strains are strongly related to India. Whole genome sequences of this
506 serotype have been recorded in three continents, Asia, Africa, and South America, where it was
507 reported as the causing agent of one of the biggest FMDV outbreaks, which occurred in
508 Argentina in 2011, affecting a total of 2,126 herds [81]. It is important to note, that there is
509 evidence of a posterior spread of these serotypes (O and A) to other countries, mainly in South
510 America, since both of them are currently found in nearly every country of the continent [26, 79].
511 However, due to the lack of whole-genome data, we were unable to further assess this spread.
512 As expected, the main host affected by serotype A was *B. taurus*. This species had an
513 important role in its viral spread [56], especially in this globalized era, where the continuous
514 increase in livestock trading markets facilitates the spread of transboundary animal diseases
515 [91]. Likewise, our phylodynamic analysis showed that the most intense host species
516 transmission route occurred from *B. taurus* to *S. caffer*, and apparently, the reverse
517 transmission is an infrequent event.

518

519 *Asia1 and SAT serotypes*

520 Whereas our results showed that serotypes O and A have spread worldwide, serotypes Asia1
521 and SATs remained non-pandemic and confined in their endemic regions [79, 92]. Since there
522 is a lack of detailed sequences data available, especially for African countries, it is important to
523 note that these results may vary with a better representation of the currently circulating virus,
524 although they support what has been previously described [59, 79, 93, 94].

525 Undoubtedly, India has been historically considered as one of the most important
526 countries for the spread and maintenance of FMDV, especially for serotypes A, and Asia1 [26,
527 55, 79, 94] Indeed, our phylogeographic analyses showed India as the most likely origin country
528 for Asia1 serotype [26, 94]. The spread of this serotype was mainly restricted to Asia [53, 55,
529 93], and characterized by local movements across the neighboring countries surrounding India,
530 China and Malaysia, where it is well known that free and unrestricted animal movements across
531 country borders may play a key role in the spread of FMDV [55, 95]. We also observed India as
532 a key center of dispersal for this serotype, which coincides with previously reported results [55].
533 The arrival of Asia1 into Turkey in 2013 represents one of the most recent and longer dispersal
534 events reported for this serotype, which was directly related to an Indian sub-lineage of the virus
535 [96]. Likewise, there have been sporadic incursions into other countries such as Greece in 1984
536 and 2000 [93], Malaysia in 1999 [31] or Turkey in 2017 [55], whose outbreaks seemed to be
537 caused also by independent sub-lineages from the rest of the outbreaks observed in these
538 regions.

539 Despite a previous study described multiple potential origins for SAT serotypes, (i.e.,
540 SAT1 in Zimbabwe and SAT2 in Kenya [48]), our root state posterior probability results
541 suggested Uganda as the most likely origin for all of them. Likewise, our phylogeographic
542 analysis also highlighted the importance of Uganda as a primary source of dispersal events to

543 different countries, where the most strongly significant routes were found from Uganda to
544 Nigeria (SAT1), from Uganda to Gaza strip (SAT2) and from Zimbabwe to Botswana (SAT3).
545 SAT serotypes (SAT1, SAT2, and SAT3) are characterized by a higher proportion of
546 local spread, limited across their endemic areas. This spread occurred mainly in southeastern
547 Africa, where nomadic pastoralism across international borders and animal trade in the sub-
548 Saharan region is one of the most practiced forms of livestock movements [48, 56, 93, 94].
549 These results complement the observations made by Bouslikhane (2015), who highlighted how
550 nomadism and transhumance play a key role in disease transmission, especially in African
551 countries.
552 Previous studies have highlighted the importance of African buffalo (*Syncerus caffer*),
553 hypothesizing that current FMDV genotypes may emerge in domesticated host species from
554 viral reservoirs maintained by this species [49, 53, 59, 94, 98–104] However, the uncertainty
555 over the involvement of African buffalo arose the need for deeper research to confirm its
556 influence in livestock outbreaks [94]. Our results coincide with the evidence mentioned in a
557 recent study by Omondi et al (2019), where cattle appeared as the most important host species
558 for the spread of FMDV, while buffalo played a secondary role. This pattern was observed not
559 only in SATs but in all serotypes studied.
560 In general, we observed considerable differences in the spatiotemporal dynamics
561 exhibited by the different serotypes. Where the serotypes with global distribution (O and A)
562 presented the most asymmetrical pattern in the annual genetic diversity in comparison with
563 (SAT and Asia1 serotypes). Cattle was observed to play a key role in the historical spread of all
564 serotypes of FMDV. Likewise, our phylodynamic analysis inferred that the transmission route
565 from cattle to buffalo was the most highly supported, pattern that was also observed for all
566 serotypes, independently of its spread potential.
567 Serotypes such as Asia1 and SATs presented local spread rates, mainly associated
568 with cattle and sheep (with special importance of buffalo in the case of SATs serotypes)

supporting previously described results (Brito et al., 2015; Omondi et al., 2019), while serotypes O and A showed long-distance spread, covering higher extensions of territory between each outbreak, which also confirms previously described information [59]. These serotypes presented the highest variety of susceptible hosts, although we speculate that the main reason for their successful long-distance spread relies mostly on the international movement of cattle and swine due to the intensive commerce between countries.

Finally, important limitations related to the use of whole genome relay in the lack of good global data, especially in African countries which remains endemically affected by five different serotypes, therefore some countries with known FMDV circulation are not part of this study. However, to reduce the bias generated by the strong unbalance of the available data in both dimensions (i.e., number of samples per country and uneven number of samples per host species), we removed all the sequences that where duplicated (i.e., represented the same outbreak multiple times), which, in the case of big outbreaks such as United Kingdom 2001/2007, Argentina 2001, and Japan 2010, accounted for hundreds of sequences representing each event. This limitation is common among phylogenic studies with no yet best alternative, this is true mainly because sample that are available hosted in public databases or from diagnostic laboratories [105]. Although whole genome sequences are increasingly proving to be a more accurate tool for phylogenetic analyses [106, 107], its high cost in comparison to studies considering partial genome results in lower availability of WGS, which became the major limitation for the construction of our dataset, resulting several countries with known reports of FMDV but lacking genetic data. Finally, it is important to highlight that, despite the nucleotide sequences encoding the capside protein VP1, VP2, and VP3 are sufficient to identify FMDV at serotype level, we preferred using WGS because of its higher accuracy in the determination of the genetic relationship between the reported cases [108].

Final remarks

595 Studies considering whole genome sequences should be preferred over partial sequence
596 research to ensure the importance of considering virus spread in its overall context
597 [53, 106, 107]. Besides, the growing awareness of the importance of using whole genome
598 sequences to assess the evolution of infectious diseases, and more specifically for RNA viruses
599 as FMDV plays a key role on the future ability to analyze the ever-increasing volume of data
600 accurately, getting closer to a real-time assessing of disease outbreaks [106]. However, the use
601 of whole genome sequences represented a limitation in our study since the lack of FMDV
602 sequences in a given country does not mean that the virus has not been circulating in that
603 country but maybe associated with technical or economic constraints, therefore interpretation
604 requires caution due to the possible introduction of sampling bias. The popularization of whole
605 genome sequencing will help not only to increase the available information about the virus, but
606 also have a direct impact on promoting new and more specific measures for disease control [24,
607 59, 109]. The result of such improvement in disease surveillance would not only be beneficial for
608 the targeted region, but also for all the areas that are directly connected (i.e., through
609 geographical limits) and indirectly (i.e., through commercial networks), including countries
610 currently considered as free zones [110].
611
612 **CONCLUSION**
613 In summary, we have seen how FMDV evolved and diversified in five species among 64
614 countries, by using a comprehensive phylodynamic approach, we characterized and compared
615 its global phylogeographic distribution at serotype scale. The phylogeographic approach used
616 here relies on the principle that evolutionary processes are better understood when a broader
617 spatiotemporal vision is available. Our results shed light on FMDV's macroevolutionary patterns
618 and spread, allowing to unravel the ancestral country of origin for each serotype as well as the
619 most important historical routes of viral dispersal, the role that the main host species played in
620 its spatial diffusion and how likely the disease is transmitted between them. The use of whole

621 genome sequences allowed us to clarify past discrepancies related to the polyphyletic nature of
622 some serotypes (i.e., SATs), previously described as monophyletic.
623 Based on our findings, we corroborate with recent advancements that have been
624 undertaken to control global distribution of major arbovirus (i.e., Dengue, yellow fever and Zika)
625 [111–113], with the need to also implement real-time genome-scale sequencing to food-animal
626 epidemics, in which metagenomics and phylogeography approaches inform epidemic responses
627 and improve control intervention strategies.
628

629 **ACKNOWLEDGEMENTS**

630 We acknowledge the Department of Population Health and Pathobiology- North Carolina State
631 University provided startup funds for G. Machado and M. Jara. SD is supported by the Fonds
632 National de la Recherche Scientifique (FNRS, Belgium). Guy Baele acknowledges support from
633 the Interne Fondsen KU Leuven / Internal Funds KU Leuven under grant agreement
634 C14/18/094.
635

636 **CONFLICT OF INTEREST**

637 The authors declare that there are no conflict of interests.
638

639 **REFERENCES**

640 1. Burrell A. Animal Disease Epidemics: Implications for Production, Policy and Trade. Outlook
641 Agric. 2002;31:151–60. doi:10.5367/000000002101294001.
642 2. Otte MJ, Nugent R, McLeod A. Transboundary animal diseases: Assessment of socio-
643 economic impacts and institutional responses. In: Food and Agriculture Organization (FAO).
644 2004. p. 119–26.
645 3. Daszak P, Cunningham AA, Hyatt AD. Anthropogenic environmental change and the
646 emergence of infectious diseases in wildlife. Acta Trop. 2001;78:103–16.

647 https://www.sciencedirect.com/science/article/pii/S0001706X00001790. Accessed 12 Oct 2018.
648 4. Kouba V. Globalization of Communicable Animal Diseases - A Crisis of Veterinary Medicine.
649 Acta Vet Brno. 2003;72:453–60. doi:10.2754/avb200372030453.
650 5. Smith KF, Sax DF, Gaines SD, Guernier V, Guégan JF. Globalization of human infectious
651 disease. Ecology. 2007;88:1903–10. doi:10.1890/06-1052.1.
652 6. Kilpatrick AM. Globalization, land use, and the invasion of West Nile virus. Science.
653 2011;334:323–7. doi:10.1126/science.1201010.
654 7. Wang T, Sun Y, Qiu H-J. African swine fever: an unprecedented disaster and challenge to
655 China. Infect Dis poverty. 2018;7:111. doi:10.1186/s40249-018-0495-3.
656 8. Stearns SC, Ebert D. Evolution in Health and Disease: Work in Progress. Q Rev Biol.
657 2001;76:417–32. doi:10.1086/420539.
658 9. Read AF, Aaby P, Antia R, Ebert D, Ewald PW, Gupta S, et al. What can evolutionary biology
659 contribute to understanding virulence? In: Evolution in Health and Disease. 1999. p. 205–16.
660 http://www.evolution.unibas.ch/ebert/publications/papers/03_book_chapters/1999_Read_in_Ste
661 arnsBOOK.PDF. Accessed 15 Jan 2019.
662 10. Trevathan W. Evolutionary medicine. In: The International Encyclopedia of Biological
663 Anthropology. Hoboken, NJ, USA: John Wiley & Sons, Inc.; 1999. p. 1–4.
664 doi:10.1002/9781118584538.ieba0534.
665 11. Galvani AP. Epidemiology meets evolutionary ecology. Trends in Ecology and Evolution.
666 2003;18:132–9. doi:10.1016/S0169-5347(02)00050-2.
667 12. Mideo N, Alizon S, Day T. Linking within- and between-host dynamics in the evolutionary
668 epidemiology of infectious diseases. Trends in Ecology and Evolution. 2008;23:511–7.
669 doi:10.1016/j.tree.2008.05.009.
670 13. Lion S, Gandon S. Spatial evolutionary epidemiology of spreading epidemics. Proc R Soc B
671 Biol Sci. 2016;283. doi:10.1098/rspb.2016.1170.
672 14. Magiorkinis G, Magiorkinis E, Paraskevis D, Ho SYW, Shapiro B, Pybus OG, et al. The

673 global spread of hepatitis C virus 1a and 1b: A phylodynamic and phylogeographic analysis.
674 PLoS Med. 2009;6:e1000198. doi:10.1371/journal.pmed.1000198.
675 15. Weaver SC, Forrester NL. Chikungunya: Evolutionary history and recent epidemic spread.
676 Antiviral Res. 2015;120:32–9. doi:10.1016/j.antiviral.2015.04.016.
677 16. Dellicour S, Lemey P, Rose R, Faria NR, Pybus OG, Vieira LFP, et al. Using Viral Gene
678 Sequences to Compare and Explain the Heterogeneous Spatial Dynamics of Virus Epidemics.
679 Mol Biol Evol. 2017;34:2563–71. https://academic.oup.com/mbe/article-
680 abstract/34/10/2563/3885213. Accessed 15 Jan 2019.
681 17. Forni D, Cagliani R, Clerici M, Sironi M. Origin and dispersal of Hepatitis e virus article.
682 Emerg Microbes Infect. 2018;7. doi:10.1038/s41426-017-0009-6.
683 18. Stephens PR, Altizer S, Smith KF, Alonso Aguirre A, Brown JH, Budischak SA, et al. The
684 macroecology of infectious diseases: a new perspective on global-scale drivers of pathogen
685 distributions and impacts. Ecol Lett. 2016;19:1159–71. doi:10.1111/ele.12644.
686 19. Jacquot M, Nomikou K, Palmarini M, Mertens P, Biek R. Bluetongue virus spread in Europe
687 is a consequence of climatic, landscape and vertebrate host factors as revealed by
688 phylogeographic inference. Proc R Soc B Biol Sci. 2017;284. doi:10.1098/rspb.2017.0919.
689 20. Lemey P, Pybus OG, Holmes EC, Grubaugh ND, Ladner JT, Rambaut A, et al. Tracking
690 virus outbreaks in the twenty-first century. Nat Microbiol. 2018;4:10–9. doi:10.1038/s41564-018-
691 0296-2.
692 21. Auguste AJ, Liria J, Forrester NL, Giambalvo D, Moncada M, Long KC, et al. Evolutionary
693 and ecological characterization of mayaro virus strains isolated during an outbreak, Venezuela,
694 2010. Emerg Infect Dis. 2015;21:1742–50. doi:10.3201/eid2110.141660.
695 22. Pigeault R, Vézilier J, Cornet S, Zélé F, Nicot A, Perret P, et al. Avian malaria: A new lease
696 of life for an old experimental model to study the evolutionary ecology of Plasmodium. Philos
697 Trans R Soc B Biol Sci. 2015;370. doi:10.1098/rstb.2014.0300.
698 23. Rogalski MA, Gowler CD, Shaw CL, Hufbauer RA, Duffy MA. Human drivers of ecological

699 and evolutionary dynamics in emerging and disappearing infectious disease systems.
700 Philosophical Transactions of the Royal Society B: Biological Sciences. 2017;372.
701 doi:10.1098/rstb.2016.0043.
702 24. Fountain-Jones NM, Pearse WD, Escobar LE, Alba-Casals A, Carver S, Davies TJ, et al.
703 Towards an eco-phylogenetic framework for infectious disease ecology. Biol Rev. 2018;93:950–
704 70. doi:10.1111/brv.12380.
705 25. Grubman MJ, Baxt B. Foot-and-mouth Disease. Clin Microbiol Rev. 2004;17:465–93.
706 http://cmr.asm.org/content/17/2/465.short. Accessed 12 Oct 2018.
707 26. Brito B, Perez AM, Mohapatra J, Subramaniam S, Pattnaik B, Rodriguez LL, et al. Dynamics
708 of widespread foot-and-mouth disease virus serotypes A, O and Asia-1 in southern Asia: A
709 Bayesian phylogenetic perspective. Transbound Emerg Dis. 2017;65:696–710.
710 https://onlinelibrary.wiley.com/doi/abs/10.1111/tbed.12791. Accessed 14 Apr 2019.
711 27. Belsham G. Distinctive features of foot-and-mouth disease virus, a member of the
712 picornavirus family; aspects of virus protein synthesis, protein processing and structure. Prog
713 Biophys Mol Biol. 1993;60:241–60.
714 https://www.sciencedirect.com/science/article/pii/007961079390016D. Accessed 15 Jan 2019.
715 28. Sobrino F, Sáiz M, Jiménez-Clavero MA, Núñez JI, Rosas MF, Baranowski E, et al. Foot-
716 and-mouth disease virus: A long known virus, but a current threat. Veterinary Research.
717 2001;32:1–30. doi:10.1051/vetres:2001106.
718 29. Brown F. The history of research in foot-and-mouth disease. Virus Res. 2003;91:3–7.
719 https://www.sciencedirect.com/science/article/pii/S016817020200268X. Accessed 3 Oct 2018.
720 30. OIE TM. Foot-And-Mouth Disease. 2009. doi:10.1146/annurev.mi.22.100168.001221.
721 31. Abdul-Hamid NF, Hussein NM, Wadsworth J, Radford AD, Knowles NJ, King DP.
722 Phylogeography of foot-and-mouth disease virus types O and A in Malaysia and surrounding
723 countries. Infect Genet Evol. 2011;11:320–8. doi:10.1016/j.meegid.2010.11.003.
724 32. Kandeil A, El-Shesheny R, Kayali G, Moatasim Y, Bagato O, Darwish M, et al.

725 Characterization of the recent outbreak of foot-and-mouth disease virus serotype SAT2 in
726 Egypt. Arch Virol. 2013;158:619–27. doi:10.1007/s00705-012-1529-y.
727 33. Ganji V, Kontham S, Pottabathula M. Understanding the Molecular Relationship between
728 Foot-and-Mouth Disease Virus Serotype O of Indian Vaccine Strain with Strains across the
729 World by. Phylogenetic Anal Int J Curr Microbiol. 2018;7:99–105. https://www.ijcmas.com/7-5-
730 2018/Vishweshwar Kumar Ganji, et al.pdf. Accessed 18 Oct 2018.
731 34. Knight-Jones T, Rushton J. The economic impacts of foot and mouth disease - What are
732 they, how big are they and where do they occur? Preventive Veterinary Medicine.
733 2013;112:162–73. doi:10.1016/j.prevetmed.2013.07.013.
734 35. Alvarez J, Goede D, Morrison R, Perez A. Spatial and temporal epidemiology of porcine
735 epidemic diarrhea (PED) in the Midwest and Southeast regions of the United States. Prev Vet
736 Med. 2016;123:155–60. doi:10.1016/j.prevetmed.2015.11.003.
737 36. Rushton J, Knight-Jones TJD. The impact of foot and mouth disease. In: FAO/OIE, Global
738 Conference on Foot and Mouth Disease Control. Food and Agriculture Organization of the
739 United Nations and the World Organisation for Animal Health; 2015. p. 205–9.
740 doi:10.1111/j.1746-692X.2004.tb00031.x.
741 37. USDA-APHIS. Planning and preparing for Foot-and-mouth disease: quick briefing. 2017.
742 https://www.aphis.usda.gov/animal_health/emergency_management/downloads/fmd-
743 briefing.pdf.
744 38. Alexandersen S, Zhang Z, Donaldson AI, Garland AJM. The pathogenesis and diagnosis of
745 foot-and-mouth disease. Journal of Comparative Pathology. 2003;129:1–36.
746 doi:10.1016/S0021-9975(03)00041-0.
747 39. IUCN/SSC ISSG. Global Invasive Species Database version 2013-1. 2018.
748 http://www.issg.org/database/welcome/. Accessed 14 Oct 2018.
749 40. Thomson GR, Bastos A. Foot-and-mouth disease. In: Infectious Diseases of Livestock.
750 Cape Town: Oxford University Press; 2004. p. 1324–65.

751 41. Orsel K, Bouma A, Dekker A, Stegeman JA, de Jong MCM. Foot and mouth disease virus
752 transmission during the incubation period of the disease in piglets, lambs, calves, and dairy
753 cows. Prev Vet Med. 2009;88:158–63. doi:10.1016/j.prevetmed.2008.09.001.
754 42. Ferguson NM, Donnelly CA, Anderson RM. Transmission intensity and impact of control
755 policies on the foot and mouth epidemic in Great Britain. Nature. 2001;413:542–8.
756 https://www.nature.com/articles/35097116. Accessed 15 Jan 2019.
757 43. Fares M a, Tully DC. The tale of a modern animal plague: tracing the evolutionary history
758 and determining the time-scale for foot and mouth disease virus. Virology. 2008;382:250–6.
759 doi:10.1016/j.virol.2008.09.011.
760 44. Schumann KR, Knowles NJ, Davies PR, Midgley RJ, Valarcher J-F, Raoufi AQ, et al.
761 Genetic characterization and molecular epidemiology of foot-and-mouth disease viruses
762 isolated from Afghanistan in 2003–2005. Virus Genes. 2008;36:401–13. doi:10.1007/s11262-
763 008-0206-4.
764 45. Priyadarshini P, Mohapatra JK, Hemadri D, Subramaniam S, Pattnaik B, Pandey L, et al.
765 Analysis of the leader proteinase (Lpro) region of type A foot-and-mouth disease virus with due
766 emphasis on phylogeny and evolution of the emerging VP359-deletion lineage from India. Virus
767 Res. 2009;141:34–46. doi:10.1016/j.virusres.2008.12.012.
768 46. Lewis-Rogers N, McClellan DA, Crandall KA. The evolution of foot-and-mouth disease virus:
769 Impacts of recombination and selection. Infect Genet Evol. 2008;8:786–98.
770 doi:10.1016/j.meegid.2008.07.009.
771 47. Lycett SJ, Tanya VN, Hall M, King D, Mazeri S, Mioulet V, et al. The evolution and
772 phylodynamics of serotype A and SAT2 foot-and-mouth disease viruses in endemic regions of
773 Africa. Sci Rep. 2019;9:5614. doi:10.1101/572198.
774 48. Omondi G, Alkhamis MA, Obanda V, Gakuya F, Sangula A, Pauszek S, et al.
775 Phylogeographical and cross-species transmission dynamics of SAT1 and SAT2 foot-and-
776 mouth disease virus in Eastern Africa. Mol Ecol. 2019;:mec.15125. doi:10.1111/mec.15125.

777 49. Hall MD, Knowles NJ, Wadsworth J, Rambaut A, Woolhouse MEJ. Reconstructing
778 geographical movements and host species transitions of foot-and-mouth disease virus serotype
779 SAT 2. MBio. 2013;4:e00591-13. doi:10.1128/mBio.00591-13.
780 50. Yoon SH, Park W, King DP, Kim H. Phylogenomics and molecular evolution of foot-and-
781 mouth disease virus. Mol Cells. 2011;31:413–21. doi:10.1007/s10059-011-0249-6.
782 51. Carrillo C, Tulman ER, Delhon G, Lu Z, Carreno A, Vagnozzi A, et al. Comparative
783 genomics of foot-and-mouth disease virus. J Virol. 2005;79:6487–504.
784 doi:10.1128/JVI.79.10.6487-6504.2005.
785 52. Cooke JN, Westover KM. Serotype-specific differences in antigenic regions of foot-and-
786 mouth disease virus (FMDV): A comprehensive statistical analysis. Infect Genet Evol.
787 2008;8:855–63. doi:10.1016/j.meegid.2008.08.004.
788 53. Lasecka-Dykes L, Wright CF, Di Nardo A, Logan G, Mioulet V, Jackson T, et al. Full
789 genome sequencing reveals new southern african territories genotypes bringing us closer to
790 understanding true variability of foot-and-mouth disease virus in Africa. Viruses. 2018;10.
791 doi:10.3390/v10040192.
792 54. Baele G, Dellicour S, Suchard MA, Lemey P, Vrancken B. Recent advances in
793 computational phylodynamics. Curr Opin Virol. 2018;31:24–32.
794 doi:10.1016/J.COVIRO.2018.08.009.
795 55. Brito B, Pauszek SJ, Eschbaumer M, Stenfeldt C, De Carvalho Ferreira HC, Vu LT, et al.
796 Phylodynamics of foot-and-mouth disease virus O/PanAsia in Vietnam 2010-2014. Vet Res.
797 2017;48:24. doi:10.1186/s13567-017-0424-7.
798 56. Di Nardo. A, Knowles N, Paton D. Combining livestock trade patterns with phylogenetics to
799 help understand the spread of foot and mouth disease in sub-Saharan Africa, the Middle East
800 and. Rev Sci Tech. 2011;30:63.
801 http://www.unitheque.com/UploadFile/DocumentPDF/L/A/OMMT-9789290448372.pdf.
802 Accessed 15 Jan 2019.

803 57. De Carvalho LMF, Santos LBL, Faria NR, De Castro Silveira W. Phylogeography of foot-
804 and-mouth disease virus serotype O in Ecuador. Infect Genet Evol. 2013;13:76–88.
805 doi:10.1016/j.meegid.2012.08.016.
806 58. Bachanek-Bankowska K, Di Nardo A, Wadsworth J, Mioulet V, Pezzoni G, Grazioli S, et al.
807 Reconstructing the evolutionary history of pandemic foot-and-mouth disease viruses: the impact
808 of recombination within the emerging O/ME-SA/Ind-2001 lineage. Sci Rep. 2018;8:14693.
809 doi:10.1038/s41598-018-32693-8.
810 59. Duchatel F, Bronsvoort M, Lycett S. Phylogeographic analysis and identification of factors
811 impacting the diffusion of Foot-and-Mouth disease virus in Africa. Front Ecol Evol. 2019;7:371.
812 60. Brito B, Pauszek SJ, Hartwig EJ, Smoliga GR, Vu LT, Dong P V., et al. A traditional
813 evolutionary history of foot-and-mouth disease viruses in Southeast Asia challenged by
814 analyses of non-structural protein coding sequences. Sci Rep. 2018;8. doi:10.1038/s41598-018-
815 24870-6.
816 61. Kumar S, Nei M, Dudley J, Tamura K. MEGA: A biologist-centric software for evolutionary
817 analysis of DNA and protein sequences. Brief Bioinform. 2008;9:299–306.
818 doi:10.1093/bib/bbn017.
819 62. Martin DP, Murrell B, Golden M, Khoosal A, Muhire B. RDP4: Detection and analysis of
820 recombination patterns in virus genomes. Virus Evol. 2015;1. doi:10.1093/ve/vev003.
821 63. Rambaut A, Lam T, Max Carvalho L, Pybus O. Exploring the temporal structure of
822 heterochronous sequences using TempEst (formerly Path-O-Gen). Virus Evol. 2016;2:vew007.
823 doi:10.1093/ve/vew007.
824 64. Murray GGR, Wang F, Harrison EM, Paterson GK, Mather AE, Harris SR, et al. The effect of
825 genetic structure on molecular dating and tests for temporal signal. Methods Ecol Evol.
826 2016;7:80–9. doi:10.1111/2041-210X.12466.
827 65. Navascués M, Depaulis F, Emerson B. Combining contemporary and ancient DNA in
828 population genetic and phylogeographical studies. Mol Ecol Resour. 2010;10:760–72.

829 doi:10.1111/j.1755-0998.2010.02895.x.

830 66. Bouckaert R, Heled J, Kühnert D, Vaughan T, Wu CH, Xie D, et al. BEAST 2: A Software

831 Platform for Bayesian Evolutionary Analysis. PLoS Comput Biol. 2014;10:e1003537.

832 doi:10.1371/journal.pcbi.1003537.

833 67. Hasegawa M, Kishino H, Yano T. Dating of the human-ape splitting by a molecular clock of

834 mitochondrial DNA. J Mol Evol. 1985;22:160–74. doi:10.1007/BF02101694.

835 68. Shapiro B, Rambaut A, Drummond AJ. Choosing appropriate substitution models for the

836 phylogenetic analysis of protein-coding sequences. academic.oup.com. 2006;23:7–9.

837 doi:10.1093/molbev/msj021.

838 69. Russel PM, Brewer BJ, Klaere S, Bouckaert RR. Model Selection and Parameter Inference

839 in Phylogenetics Using Nested Sampling. Syst Biol. 2019;68:219–33.

840 doi:10.1093/sysbio/syy050.

841 70. Drummond AJ, Ho SYW, Phillips MJ, Rambaut A. Relaxed phylogenetics and dating with

842 confidence. PLoS Biol. 2006;4:e88. doi:10.1371/journal.pbio.0040088.

843 71. Drummond A, Rambaut A, Shapiro B, Pybus OG. Bayesian coalescent inference of past

844 population dynamics from molecular sequences. Mol Biol Evol. 2005;22:1185–92.

845 doi:10.1093/molbev/msi103.

846 72. Rambaut AR, Drummond ALJ, Dong X, Baele G, Suchard M. Posterior Summarization in

847 Bayesian Phylogenetics Using Tracer 1 . 7. Syst Biol. 2018;67:901–4.

848 doi:10.1093/sysbio/syy032.

849 73. Rambaut A. FigTree-version 1.4. 3, a graphical viewer of phylogenetic trees. 2017.

850 74. Lemey P, Rambaut A, Drummond AJ, Suchard MA. Bayesian Phylogeography Finds Its

851 Roots. PLoS Comput Biol. 2009;5:e1000520. doi:10.1371/journal.pcbi.1000520.

852 75. Drummond AJ, Bouckaert RR. Bayesian evolutionary analysis with BEAST. Cambridge

853 University Press; 2015.

854 76. Bielejec F, Baele G, Vrancken B, Suchard M, Rambaut A, Lemey P. SpreaD3: interactive

855 visualization of spatiotemporal history and trait evolutionary processes. Mol Biol Evol.
856 2016;33:2167–9. https://academic.oup.com/mbe/article-abstract/33/8/2167/2579258. Accessed
857 15 Jan 2019.
858 77. Hemadri D, Tosh C, Sanyal A, Venkataramanan R. Emergence of a new strain of type O
859 Foot-and-mouth disease virus: Its phylogenetic and evolutionary relationship with the PanAsia
860 pandemic strain. Virus Genes. 2002;25:23–34. doi:10.1023/A:1020165923805.
861 78. Knowles NJ, Samuel AR, Davies PR, Midgley RJ, Valarcher J-F. Pandemic strain of foot-
862 and-mouth disease virus serotype O. Emerg Infect Dis. 2005;11:1887–93.
863 doi:10.3201/eid1112.050908.
864 79. Rweyemamu M, Roeder P, Mackay D, Sumption K, Brownlie J, Leforban Y, et al.
865 Epidemiological Patterns of Foot-and-Mouth Disease Worldwide. Transbound Emerg Dis.
866 2008;55:57–72. doi:10.1111/j.1865-1682.2007.01013.x.
867 80. Perez AM, Ward MP, Carpenter TE. Control of a foot-and-mouth disease epidemic in
868 Argentina. Prev Vet Med. 2004;65:217–26.
869 81. Perez AM, Ward MP, Carpenter TE. Epidemiological investigations of the 2001 foot-and-
870 mouth disease outbreak in Argentina. Vet Rec. 2004;154:777–82.
871 https://veterinaryrecord.bmj.com/content/154/25/777.short. Accessed 8 Mar 2019.
872 82. Thompson D, Muriel P, Russell D, Osborne P, Bromley A, Rowland M, et al. Economic costs
873 of the foot and mouth disease outbreak in the United Kingdom in 2001. Rev Sci Tech.
874 2002;21:675–87. https://europepmc.org/abstract/med/12523706. Accessed 15 Jan 2019.
875 83. Gloster J, Paton DJ, Hutchings GH, King DP, Ferris NP, Haydon DT, et al. Molecular
876 Epidemiology of the Foot-and-Mouth Disease Virus Outbreak in the United Kingdom in 2001. J
877 Virol. 2006;80:11274–82. doi:10.1128/jvi.01236-06.
878 84. Melo EC, Saraiva V, Studillo V. Review of the status of foot and mouth disease in countries
879 of South America and approaches to control and eradication. Rev Sci Tech Int des épizooties.
880 2002;21:429–33. doi:10.20506/rst.21.3.1350.

881 85. Huang CC, Lin YL, Huang TS, Tu WJ, Lee SH, Jong MH, et al. Molecular characterization of
882 foot-and-mouth disease virus isolated from ruminants in Taiwan in 1999-2000. Vet Microbiol.
883 2001;81:193–205. doi:10.1016/S0378-1135(01)00308-X.
884 86. Dunn CS, Donaldson AI. Natural adaption to pigs of a Taiwanese isolate of foot-and-mouth
885 disease virus. Vet Rec. 1997;141:174–5. doi:10.1136/vr.141.7.174.
886 87. Yang PC, Chu RM, Chung WB, Sung HT. Epidemiological characteristics and financial costs
887 of the 1997 foot-and-mouth disease epidemic in Taiwan. Vet Rec. 1999;145:731–4.
888 https://veterinaryrecord.bmj.com/content/145/25/731.short. Accessed 12 Jul 2019.
889 88. Knowles NJ, Samuel AR, Davies PR, Kitching RP, Donaldson AI. Outbreak of foot-and-
890 mouth disease virus serotype O in the UK caused by a pandemic strain. Vet Rec.
891 2001;148:258–9. http://www.ncbi.nlm.nih.gov/pubmed/11292084. Accessed 12 Jul 2019.
892 89. Sangare O, Bastos AD, Marquardt O, Venter EH, Vosloo W, Thomson GR. Molecular
893 epidemiology of serotype O foot-and-mouth disease virus with emphasis on West and South
894 Africa. Virus Genes. 2001;22:345–51.
895 https://link.springer.com/article/10.1023/A:1011178626292. Accessed 12 Jul 2019.
896 90. Pluimers FH, Akkerman AM, van der Wal P, Dekker A, Bianchi A. Lessons from the foot and
897 mouth disease outbreak in The Netherlands in 2001. Rev Sci Tech. 2002;21:711–21.
898 https://pdfs.semanticscholar.org/ada9/a1b0ecd88ea85df19e53b462fd897bff4b11.pdf. Accessed
899 12 Jul 2019.
900 91. Cartín-Rojas A. Transboundary animal diseases and international trade. In: International
901 Trade from Economic and Policy Perspective. 2012. p. 143–66.
902 https://books.google.com/books?hl=es&lr=&id=AO6dDwAAQBAJ&oi=fnd&pg=PA143&dq=Trans
903 boundary+animal+diseases+and+international+trade&ots=EFgRQFP16_&sig=7zwIV71w7VMu
904 N840ZcDs26yWhm0. Accessed 12 Jul 2019.
905 92. Kitching RP. Global Epidemiology and Prospects for Control of Foot-and-Mouth Disease. In:
906 Foot-and-Mouth-Disease Virus. Heidelberg, Berlin: Springer-Verlag; 2005. p. 133–48.

907 https://link.springer.com/content/pdf/10.1007/3-540-27109-0_6.pdf. Accessed 12 Jul 2019.

908 93. Jamal SM, Belsham GJ. Foot-and-mouth disease: past, present and future. Vet Res.

909 2013;44:116. doi:10.1186/1297-9716-44-116.

910 94. Brito B, Rodriguez L, Hammond J, Pinto J, Perez A. Review of the Global Distribution of

911 Foot-and-Mouth Disease Virus from 2007 to 2014. Transboundary and Emerging Diseases.

912 2015;64:316–32. doi:10.1111/tbed.12373.

913 95. Subramaniam S, Pattnaik B, Sanyal A, Mohapatra JK, Pawar SS, Sharma GK, et al. Status

914 of Foot-and-mouth Disease in India. Transbound Emerg Dis. 2013;60:197–203.

915 doi:10.1111/j.1865-1682.2012.01332.x.

916 96. Upadhyaya S, Ayelet G, Paul G, King DP, Paton DJ, Mahapatra M. Genetic basis of

917 antigenic variation in foot-and-mouth disease serotype A viruses from the Middle East. Vaccine.

918 2014;32:631–8. doi:10.1016/j.vaccine.2013.08.102.

919 97. Bouslikhane M. Cross border movements of animals and animal products and their

920 relevance to the epidemiology of animals disease in Africa. OIE Africa Regional Commision.;

921 2015. https://pdfs.semanticscholar.org/3502/9521c392e33c47c1d7c039f9a172fc132008.pdf.

922 Accessed 21 Mar 2019.

923 98. Dion E, VanSchalkwyk L, Lambin EF. The landscape epidemiology of foot-and-mouth

924 disease in South Africa: A spatially explicit multi-agent simulation. Ecol Modell. 2011;222:2059–

925 72. doi:10.1016/j.ecolmodel.2011.03.026.

926 99. Vosloo W, Bastos AD, Kirkbride E, Esterhuysen JJ, van Rensburg DJ, Bengis RG, et al.

927 Persistent infection of African buffalo (Syncerus caffer) with SAT-type foot-and-mouth disease

928 viruses: rate of fixation of mutations, antigenic change and interspecies transmission. J Gen

929 Virol. 1996;77:1457–67. doi:10.1099/0022-1317-77-7-1457.

930 100. Thomson GR, Vosloo W, Bastos AD. Foot and mouth disease in wildlife. Virus Res.

931 2003;91:145–61. doi:10.1016/s0168-1702(02)00263-0.

932 101. Michel AL, Bengis RG. The Afican buffalo: A villain for inter-species spread of infectious

933 diseases in southern Africa. OpenJournals Publishing; 2012.
934 http://www.scielo.org.za/scielo.php?script=sci_arttext&pid=S0030-24652012000200006.
935 Accessed 5 Jul 2019.
936 102. Bronsvoort BMDC, Parida S, Handel I, McFarland S, Fleming L, Hamblin P, et al.
937 Serological survey for foot-and-mouth disease virus in wildlife in eastern Africa and estimation of
938 test parameters of a nonstructural protein enzyme-linked immunosorbent assay for buffalo. Clin
939 Vaccine Immunol. 2008;15:1003–11. doi:10.1128/CVI.00409-07.
940 103. Ayebazibwe C, Mwiine FN, Tjørnehøj K, Balinda SN, Muwanika VB, Ademun Okurut AR, et
941 al. The role of African buffalos (syncerus caffer) in the maintenance of foot-and-mouth disease
942 in Uganda. BMC Vet Res. 2010;6:54. doi:10.1186/1746-6148-6-54.
943 104. Dhikusooka MT, Tjørnehøj K, Ayebazibwe C, Namatovu A, Ruhweza S, Siegismund HR, et
944 al. Foot-and-mouth disease virus serotype SAT 3 in long-horned ankole Calf, Uganda. Emerg
945 Infect Dis. 2015;21:111–4. doi:10.3201/eid2101.140995.
946 105. Frost SDW, Pybus OG, Gog JR, Viboud C, Bonhoeffer S, Bedford T. Eight challenges in
947 phylodynamic inference. Epidemics. 2015;10:88–92. doi:10.1016/j.epidem.2014.09.001.
948 106. Dudas G, Bedford T. The ability of single genes vs full genomes to resolve time and space
949 in outbreak analysis. BiorXiv. 2019;:27. doi:10.1101/582957.
950 107. Gilchrist CA, Turner SD, Riley MF, Petri WA, Hewlett EL. Whole-genome sequencing in
951 outbreak analysis. Clin Microbiol Rev. 2015;28:541–63. doi:10.1128/CMR.00075-13.
952 108. Mason PW, Pacheco JM, Zhao QZ, Knowles NJ. Comparisons of the complete genomes
953 of Asian, African and European isolates of a recent foot-and-mouth disease virus type O
954 pandemic strain (PanAsia). J Gen Virol. 2003;84:1583–93. doi:10.1099/vir.0.18669-0.
955 109. Schrag SJ, Wiener P. Emerging infectious disease: what are the relative roles of ecology
956 and evolution. Trends Ecol Evol. 1995;10:319–24.
957 https://www.sciencedirect.com/science/article/pii/S0169534700891181. Accessed 17 Jan 2019.
958 110. King D, Di Nardo A, Henstock M. OIE/FAO Foot-and-Mouth Disease Reference Laboratory

959 Network: Annual report 2017. 2016;:91.

960 111. Thézé J, Li T, du Plessis L, Bouquet J, Kraemer MU, Somasekar S, et al. Genomic

961 Epidemiology Reconstructs the Introduction and Spread of Zika Virus in Central America and

962 Mexico. Cell host Microbe. 2018;23:1–10.

963 https://www.sciencedirect.com/science/article/pii/S193131281830218X. Accessed 12 Jul 2019.

964 112. Faria NR, Kraemer MU, Hill S, De Jesus JG, De Aguiar RS, Iani FC, et al. Genomic and

965 epidemiological monitoring of yellow fever virus transmission potential. BiorXiv. 2018.

966 113. Messina J, Brady O, Golding N, Kraemer MUG, Wint GRW, Ray SE, et al. The current and

967 future global distribution and population at risk of dengue. Nat Microbiol. 2019;in press.

968 https://www.nature.com/articles/s41564-019-0476-8. Accessed 12 Jul 2019.

969

970 **SUPPLEMENTARY MATERIAL**

971

972 **TABLE S1.** Sample information for all Foot and Mouth Disease virus complete genome

973 sequences used in this study.

974

975 **TABLE S2.** Root-to-tip regression analyses of phylogenetic temporal signal. Correlation and

976 determination coefficient (R2) were estimated with TempEst (Rambaut et al. 2016). P-values

977 were calculated using the approach of Murray et al. (2016) and were based on 1,000 random

978 permutations of the sequence sampling dates (Navascuès et al. 2010).

979

980 **TABLE S3.** Number of sequences and serotypes per country.

981

982 **Fig. S1** Spatial distribution of Foot-and-mouth disease virus showing the number of serotypes

983 per country.

984

985 **Fig. S2** Reconstructed Bayesian Coalescent Skyline plots (BSP) of FMDV serotypes. The
986 median estimated of the effective population size through time are represented by the dark blue.
987 The 95% highest posterior density confidence intervals are marked in blue.
988
989 **Video S1.** Reconstructed spatiotemporal diffusion of FMD serotype O spread, where diameters
990 of the colored circles are proportional to the square root of the number of MCC branches,
991 maintaining a particular location state at each time period. The color of the branches represents
992 the age of the internal nodes, where darker red colors represent older spread events, this
993 visualization match with the main time bar on top of the video.
994
995 **Video S2.** Reconstructed spatiotemporal diffusion of FMD serotype A spread, where diameters
996 of the colored circles are proportional to the square root of the number of MCC branches,
997 maintaining a particular location state at each time period. The color of the branches represents
998 the age of the internal nodes, where darker red colors represent older spread events, this
999 visualization match with the main time bar on top of the video.
1000
1001 **Video S3.** Reconstructed spatiotemporal diffusion of FMD serotype Asia1 spread, where
1002 diameters of the colored circles are proportional to the square root of the number of MCC
1003 branches, maintaining a particular location state at each time period. The color of the branches
1004 represents the age of the internal nodes, where darker red colors represent older spread
1005 events, this visualization match with the main time bar on top of the video.
1006
1007 **Video S4.** Reconstructed spatiotemporal diffusion of FMD serotype SAT1 spread, where
1008 diameters of the colored circles are proportional to the square root of the number of MCC
1009 branches, maintaining a particular location state at each time period. The color of the branches

represents the age of the internal nodes, where darker red colors represent older spread events, this visualization match with the main time bar on top of the video.

Video S5. Reconstructed spatiotemporal diffusion of FMD serotype SAT2 spread, where diameters of the colored circles are proportional to the square root of the number of MCC branches, maintaining a particular location state at each time period. The color of the branches represents the age of the internal nodes, where darker red colors represent older spread events, this visualization match with the main time bar on top of the video.

Video S6. Reconstructed spatiotemporal diffusion of FMD serotype SAT3 spread, where diameters of the colored circles are proportional to the square root of the number of MCC branches, maintaining a particular location state at each time period. The color of the branches represents the age of the internal nodes, where darker red colors represent older spread events, this visualization match with the main time bar on top of the video.